AD NUMBER

AD803132

LIMITATION CHANGES

TO:

Approved for public release; distribution is unlimited.

FROM:

**Distribution authorized to U.S. Gov't. agencies and their contractors;
Administrative/Operational Use; NOV 1966. Other requests shall be referred to Arnold Engineering Development Center, Arnold AFB, TN.**

AUTHORITY

AEDC ltr 12 Feb 1973

AEDC-TR-66-238

EXPLOSIVELY DRIVEN SHOCK TUBES

[redacted]

E. T. Moore, Jr.
Physics International Company
San Leandro, California

November 1966

Contract F 40(600)-1139

ARNOLD ENGINEERING DEVELOPMENT CENTER
AIR FORCE SYSTEMS COMMAND
ARNOLD AIR FORCE STATION, TENNESSEE

NOTICES

When U. S. Government drawings specifications, or other data are used for any purpose other than a definitely related Government procurement operation, the Government thereby incurs no responsibility nor any obligation whatsoever, and the fact that the Government may have formulated, furnished, or in any way supplied the said drawings, specifications, or other data, is not to be regarded by implication or otherwise, or in any manner licensing the holder or any other person or corporation, or conveying any rights or permission to manufacture, use, or sell any patented invention that may in any way be related thereto.

Qualified users may obtain copies of this report from the Defense Documentation Center.

References to named commercial products in this report are not to be considered in any sense as an endorsement of the product by the United States Air Force or the Government.

EXPLOSIVELY DRIVEN SHOCK TUBES

PIFR-037

E. T. Moore, Jr.
Physics International Company
San Leandro, California

FOREWORD

The work reported herein was sponsored by Arnold Engineering Development Center (AEDC), Air Force Systems Command (AFSC), Arnold Air Force Station, Tennessee, under Program Element 62410034/7778, Task 777807. Technical monitoring of the contract was performed by Mr. M. L. Laster, Technical Monitor, AEDC, and Dr. Hans K. Doetsch, Technical Advisor to the DCS/Research, AEDC.

The contract effort was conducted from August 15, 1965, to May 15, 1966, by personnel of Physics International Company, San Leandro, California, under Contract AF40(600)-1139. The manuscript was submitted for publication on November 2, 1966.

The author is grateful for computer calculations of shock-tube flow furnished by Mr. Glen Norfleet, Supervisor, Shock Tunnel Section, von Kármán Facility, ARO, Inc., Arnold Air Force Station, Tennessee.

The reproducibles used in the reproduction of this report were supplied by the author.

This technical report has been reviewed and is approved.

Marion L. Laster
Aerospace Engineer
Research Division
Directorate of Plans
and Technology

Donald R. Eastman
Acting Director
Directorate of Plans and
Technology

ABSTRACT

This report summarizes the analytical and experimental effort that demonstrates the feasibility of using an explosive driver to produce strong planar shock waves at constant velocity in air. Shock-tube performance using an explosive driver was experimentally investigated for initial test gas pressures ranging from 0.1 mm Hg to 1000 mm Hg. The best performance in terms of constant shock velocities was 46,900 ft/sec obtained in 1.0 mm Hg of air.

CONTENTS

LIST OF ILLUSTRATIONS

TABLES

SECTION I
INTRODUCTION

The varied objectives of current and projected space programs require that hypersonic flow phenomena be studied for vastly different flight conditions. For example, the plunging re-entry of a hardened ballistic system carries it to moderate velocities at quite low altitudes. On the other hand, fragile interplanetary vehicles will experience extended periods at extremely high velocities and altitudes. For many years shock tubes and shock tunnels have been used quite successfully to simulate many of the flow properties of high-speed flight. Their ability to produce a relatively wide range of gas flow properties is well recognized. However, because of the current interest in an ever-expanding range of flight conditions, it is imperative that new methods be developed that extend the capabilities of these techniques.

For the past three and a half years, Physics International has been engaged in a continuing program of research aimed at the development of explosively driven hypervelocity gas guns (Refs. 1, 2). These guns utilize an explosive driver designed to convert the chemical energy of an explosive into kinetic and internal energy of a light gas. The major objective has been to use the resultant high-enthalpy gas to accelerate a projectile. The purpose of the present research was to determine the feasibility of using an explosive driver, as developed for the launching of projectiles, to drive a high-performance shock tube. This report summarizes the analytical and experimental effort expended to realize this feasibility. The operational characteristics of the explosive driver and the theoretical performance estimates of a shock tube using this driver are presented in Section II. A two-stage shock tube was designed whose experimental performance was investigated for initial test gas pressures ranging from 0.1 mm Hg to 1000 mm Hg. The results of the experimental program are given in Section III. The experimentally observed shock wave and particle velocities were

found to agree closely with theoretically predicted values for initial test gas pressures above 10 mm Hg. While slightly higher than predicted, the highest constant shock velocity was 46,900 ft/sec obtained in 1.0 mm Hg of air. A summary of the present state of development and recommendations for future research are found in Section IV.

SECTION II
DEVELOPMENT OF AN EXPLOSIVELY DRIVEN SHOCK TUBE

In order to integrate the explosive driver into a high-performance shock tube, it was necessary to analyze the shock tube performance that could be expected based on the flow conditions produced in the driver gas. These aspects of the driver and shock tube are described in the sections that follow. Also included are a physical description of the complete shock tube and of the basic instrumentation used to diagnose experimental performance.

A. OPERATIONAL CHARACTERISTICS OF THE EXPLOSIVE DRIVER

The operation of the explosive driver is shown schematically in Figure 1. A thin-walled steel cylinder serves as a pressure tube that contains the driver gas. This tube is surrounded by a concentric cylinder of high explosive. After the explosive is detonated, the detonation front propagates along the outside of the pressure tube. The resulting pressure accelerates the walls of the pressure tube in toward the axis, sealing the tube and forming a conical-shaped piston, Figure 1b. The motion of this piston generates a shock wave that moves out ahead of the detonation front and into the stationary column of driver gas, Figure 1c.

The conservation of momentum across the shock front gives the pressure P_2 in the gas behind the shock wave

$$P_2 = P_1 + \rho_1 U_2 S \tag{1}$$

in terms of the gas velocity U_2 of the gas behind the shock wave, the velocity of the shock wave S, the pressure P_1, and density ρ_1 of the gas in front of the shock wave. For the magnitude of pressures P_2 being considered, the pressure P_1 can be neglected. The gas behind the shock wave will assume the velocity of the conical-shaped piston, which

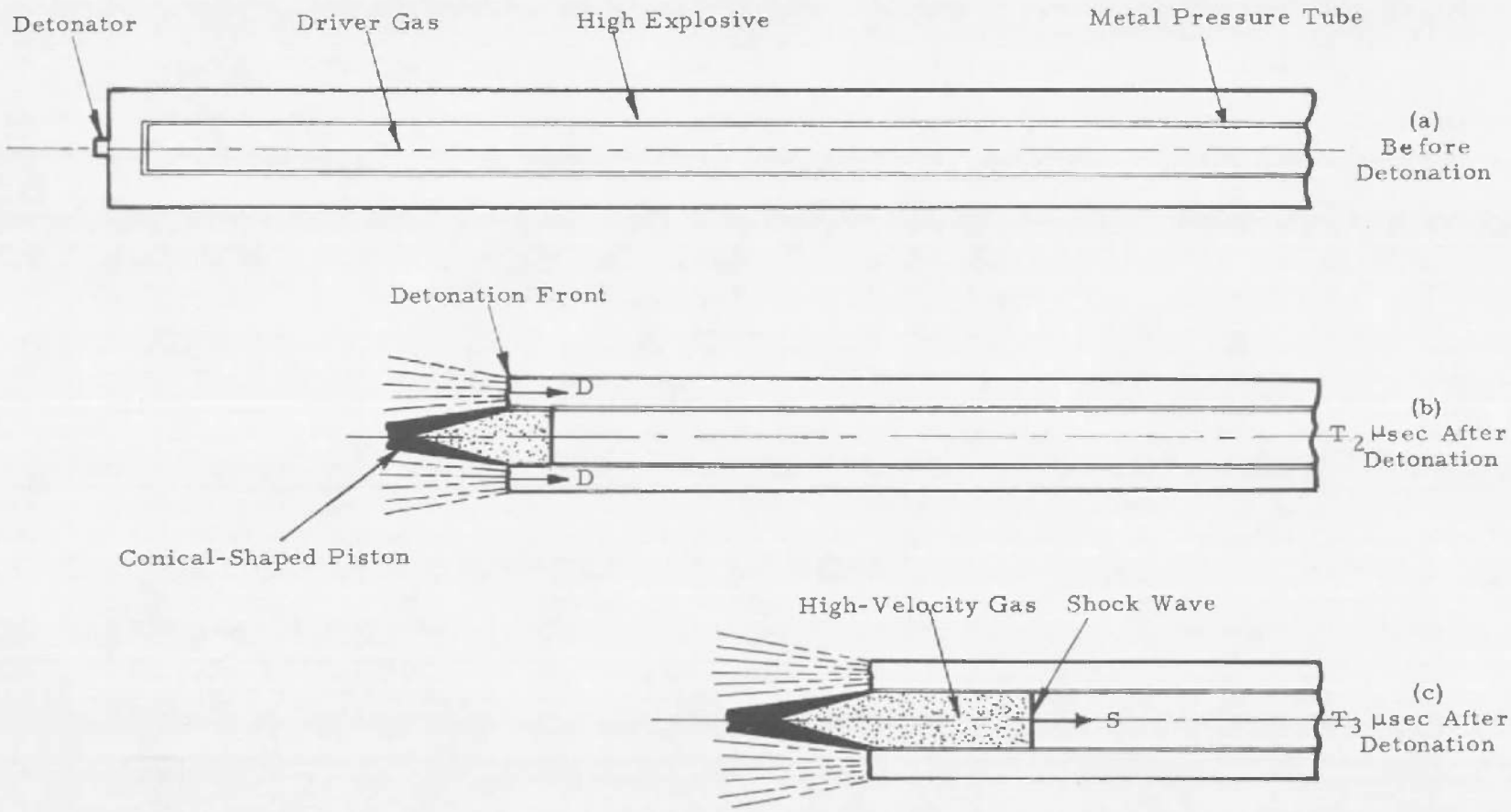

Fig. 1 Operation of an Explosive Driver

under steady-state conditions will be identical to the detonation velocity D of the high explosive. Equation (1) now becomes

$$P_2 = \rho_1 DS \tag{2}$$

Conservation of mass across the shock front yields

$$S = \frac{\frac{\rho_2}{\rho_1}}{\frac{\rho_2}{\rho_1} - 1} D \quad \text{or} \quad \frac{\eta}{\eta - 1} D \tag{3}$$

where $\eta = \rho_2/\rho_1$ is defined as the compression. If the driver gas is assumed to be an ideal gas, the maximum compression for a single strong shock can be expressed solely in terms of the ratio of specific heats of the gas, or

$$\eta = \frac{\gamma + 1}{\gamma - 1} \tag{4}$$

where $\gamma = c_p/c_v$. The shock velocity, Equation (3), now becomes

$$S = \frac{\gamma + 1}{2} D \tag{5}$$

and the pressure in the gas behind the shock wave is given by

$$P_2 = \rho_1 \frac{\gamma + 1}{2} D^2 \tag{6}$$

The versatility of the explosive driver is demonstrated by the latter relation, Equation (6). The pressure in the gas can be controlled over a considerable range of gases (γ), loading densities (ρ), and high explosives (D).

The model presented above to describe the operation of the explosive driver is highly idealized and has been used to facilitate calculations. For example, the radial expansion of the pressure tube as a result of the shock wave has not been included, and the early stages of shock formation (when the shock is lagging behind the detonation front) have not been described. These phenomena are sufficiently complex to make theoretical descriptions extremely difficult and beyond the scope of this report.

Because the explosive driver generates a highly reproducible wave pattern, it is unnecessary to describe individual experiments here. The wave diagram shown in Figure 2 summarizes the performance of the explosive drivers used in this study. The zero time of this figure is based on the time at which an electronic pulse is applied to the explosive firing system. The difference between zero time and the point at which the detonation wave intersects the time axis is the delay time t_D required for the detonator and booster explosives to initiate the nitromethane in the driver ($\approx$ 11 μsec).

As the detonation wave propagates along the outside of the pressure tube, the tube is accelerated in toward the axis and forms a conical-shaped piston. The motion of this piston produces a shock wave in the driver gas that soon overtakes the detonation front. The time and position at which this occurs is designated as (t_0, x_0) in Figure 2. Since the time $t_0 - t_D$ represents the time required to form the piston, the point (t_0, x_0) now becomes the origin of a wave pattern describing the instantaneous acceleration of the piston to a constant velocity of 21,063 ft/sec (the detonation velocity observed for the nitromethane). If the helium driver gas is assumed to behave as an ideal gas whose ratio of specific heats γ is equal to 5/3, then the velocity of the shock is related to the detonation velocity through the relation

$$S = \frac{\gamma + 1}{2} D$$

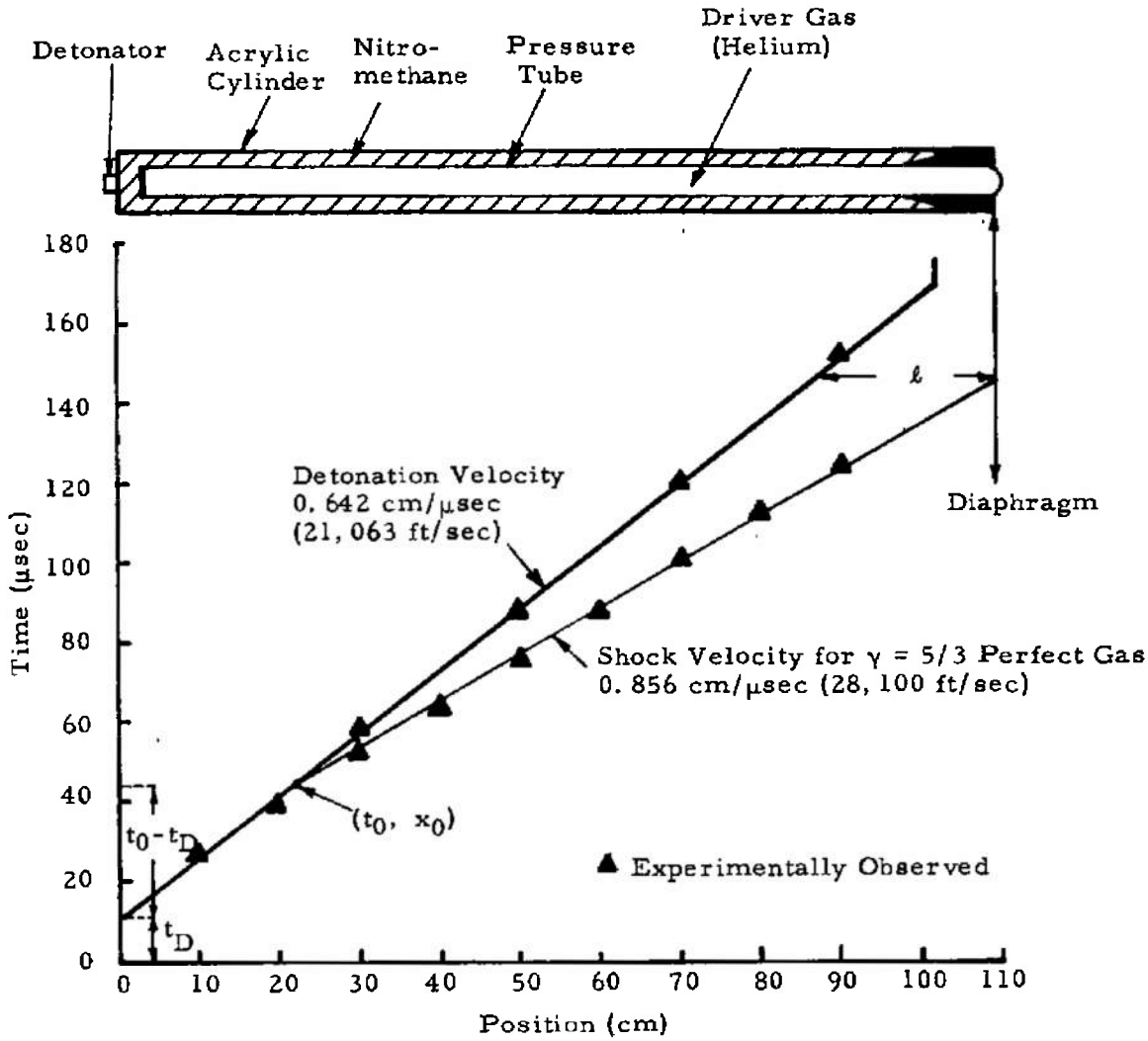

Fig. 2 Characteristic Wave Diagram of the 4000-atm Explosive Driver

developed as Equation (5) above. For γ = 5/3 and a detonation velocity D of 21,063 ft/sec, this expression yields a shock velocity of 28,100 ft/sec, which is shown in Figure 2 as a solid line. While the observed shock velocity is not constant (see Figure 2), its proximity to that predicted by an ideal gas model is sufficient to encourage further use of the model to calculate the properties of the gas behind the shock wave. By the time the shock wave encounters the diaphragm, a reservoir of high-enthalpy gas has been created between the diaphragm and piston. The length of this reservoir is denoted as ℓ in Figure 2. The properties of the shocked gas in this reservoir are listed in Table I.

The fact that the observed shock wave seems to decelerate slightly as it proceeds down the pressure tube may be attributed to the previously mentioned radial expansion that occurs in the pressure tube

TABLE I
PROPERTIES OF THE SHOCKED DRIVER GAS OF THE STANDARD EXPLOSIVE DRIVER

Length of shocked gas	21 cm
Velocity	0.642 cm/μsec (21,063 ft/sec)
Pressure	3980 atm
Density *	0.0312 g/cm^3
Internal Energy Density *	20,600 J/g
Kinetic Energy Density	20,600 J/g
Specific Enthalpy *	34,400 J/g
Temperature *	6600°K

*As calculated assuming an ideal gas with ratio of specific heats (γ) of 5/3.

after the shock wave passes. The expansion presents continuously changing conditions to the detonation wave front. The explosive must now accelerate the pressure tube from progressively larger radii toward the driver gas, whose mass per unit length is gradually increasing.

B. PERFORMANCE ESTIMATES OF THE SHOCK TUBE

Computer calculations* were used to predict the performance of a shock tube driven by a 4000-atm explosive driver. These calculations solve the one-dimensional inviscid fluid relations that describe the unsteady wave system of a shock tube. Gas flow properties were calculated for various test parameters such as initial test gas pressure and the area ratio between the driver and driven sections. For these calculations, the equation of state of air was based on the data of Hilsenrath and Klein (Ref. 3), while the helium driver gas was assumed to be ideal.

The shock-tube geometry chosen for study is shown in Figure 3 The characteristic wave pattern generated by this configuration is also shown in this figure. The symbols and nomenclature of the wave diagram correspond to normal shock-tube notation and will be used throughout this report. It should be noted that an area change is located at the diaphragm. The wave diagram of Figure 3 assumed that the steady expansion due to the area change occurs instantaneously at the diaphragm, i.e., the nozzle length is zero. Unusual as it seems, the purpose of this area change is to degrade the performance of the explosively driven shock tube. This was necessary in order to compare experimental results with theoretical predictions based on currently available thermodynamic data of air.

The theoretical performance of a shock tube driven by a 4000-atm explosive driver is summarized in Figures 4, 5, and 6. The Mach number M_{s8} of the shock wave entering the test gas, the pressure P_7

*The computer calculations were provided by Mr. Glen Norfleet of ARO, Incorporated.

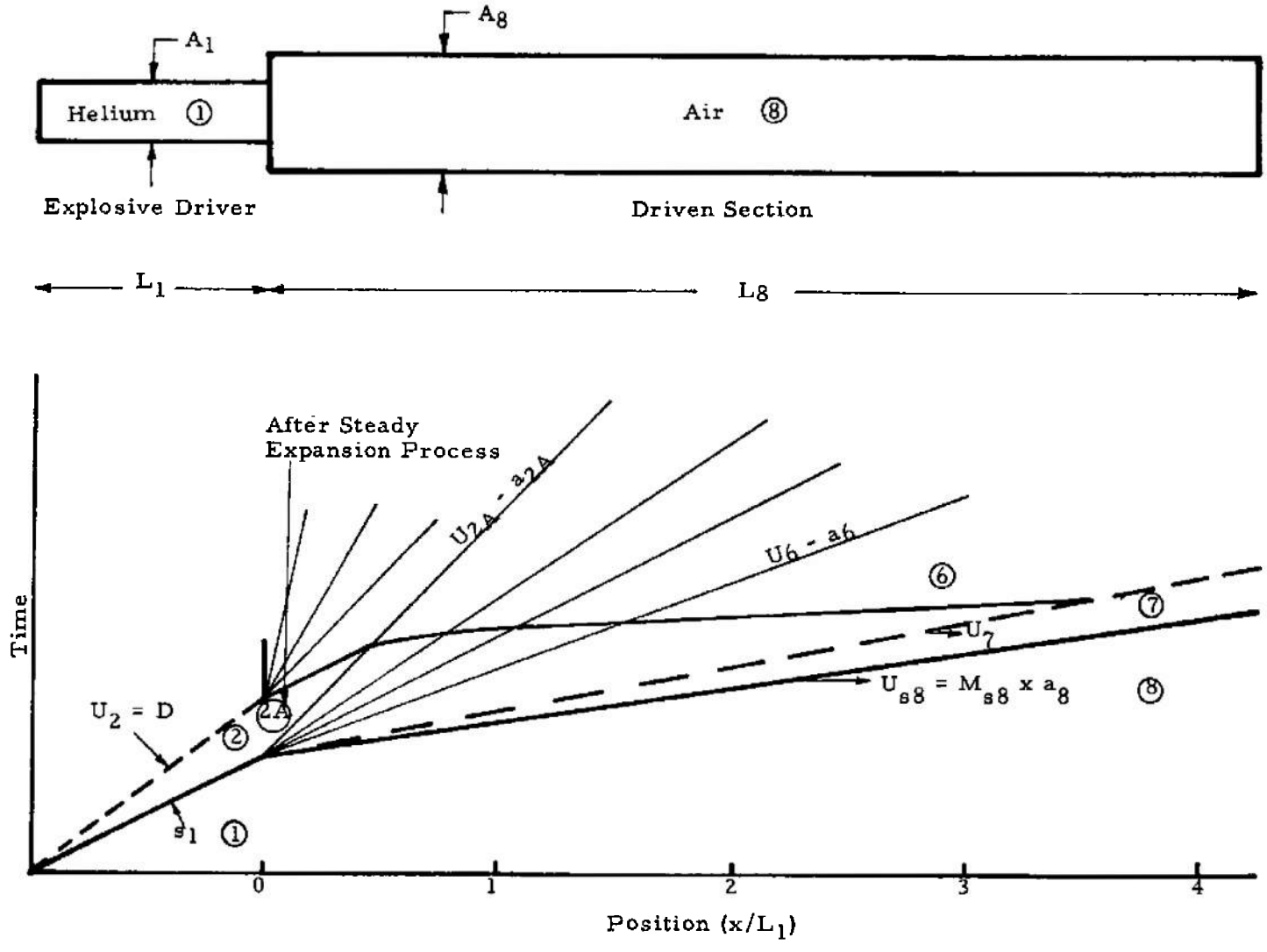

Fig. 3 Characteristic Wave Diagram of Explosively Driven Shock Tube

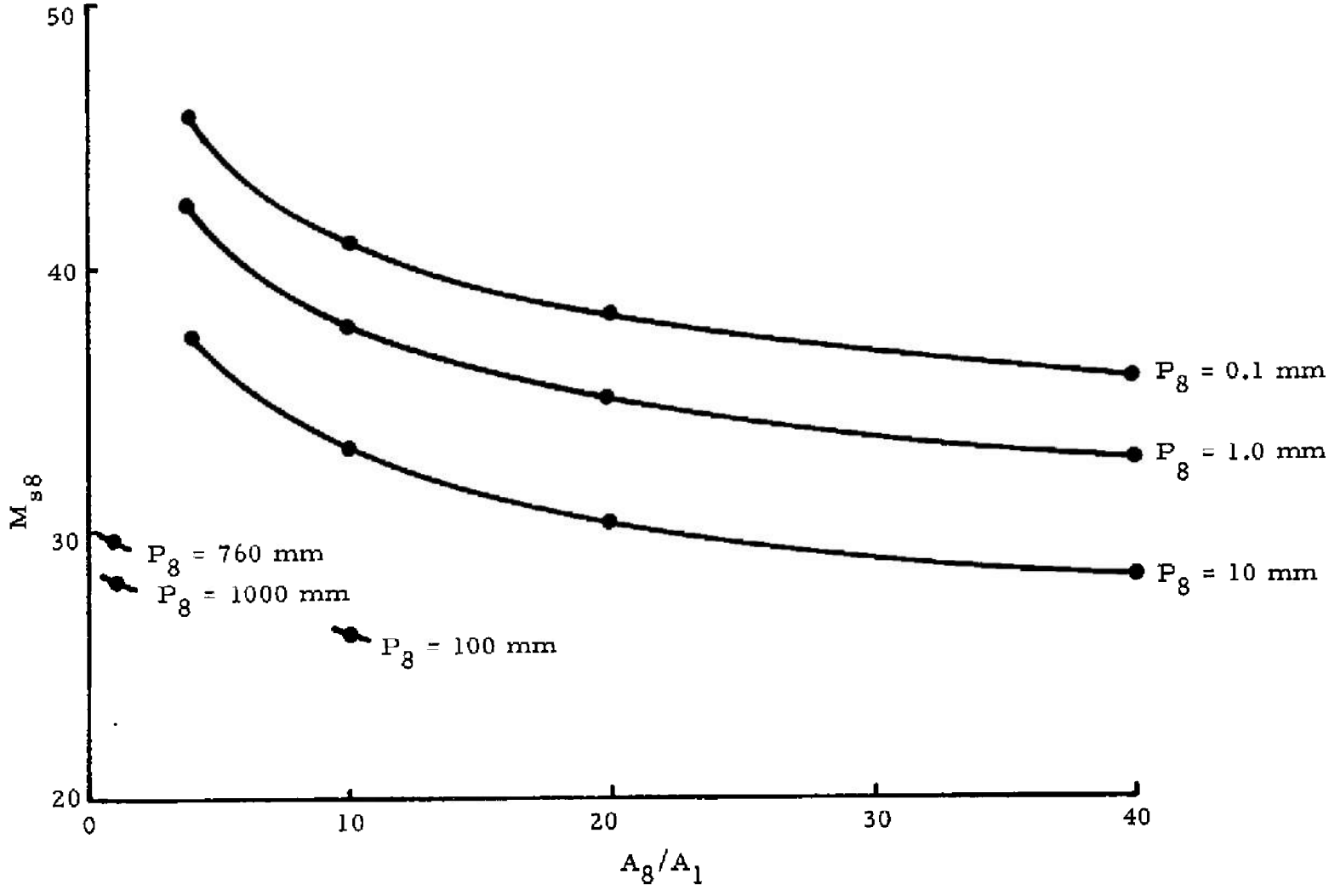

Fig. 4 Shock Mach Number Produced in Air for Various Shock Tube Test Parameters, 4000-atm Explosive Driver (Air data from Ref. 3)

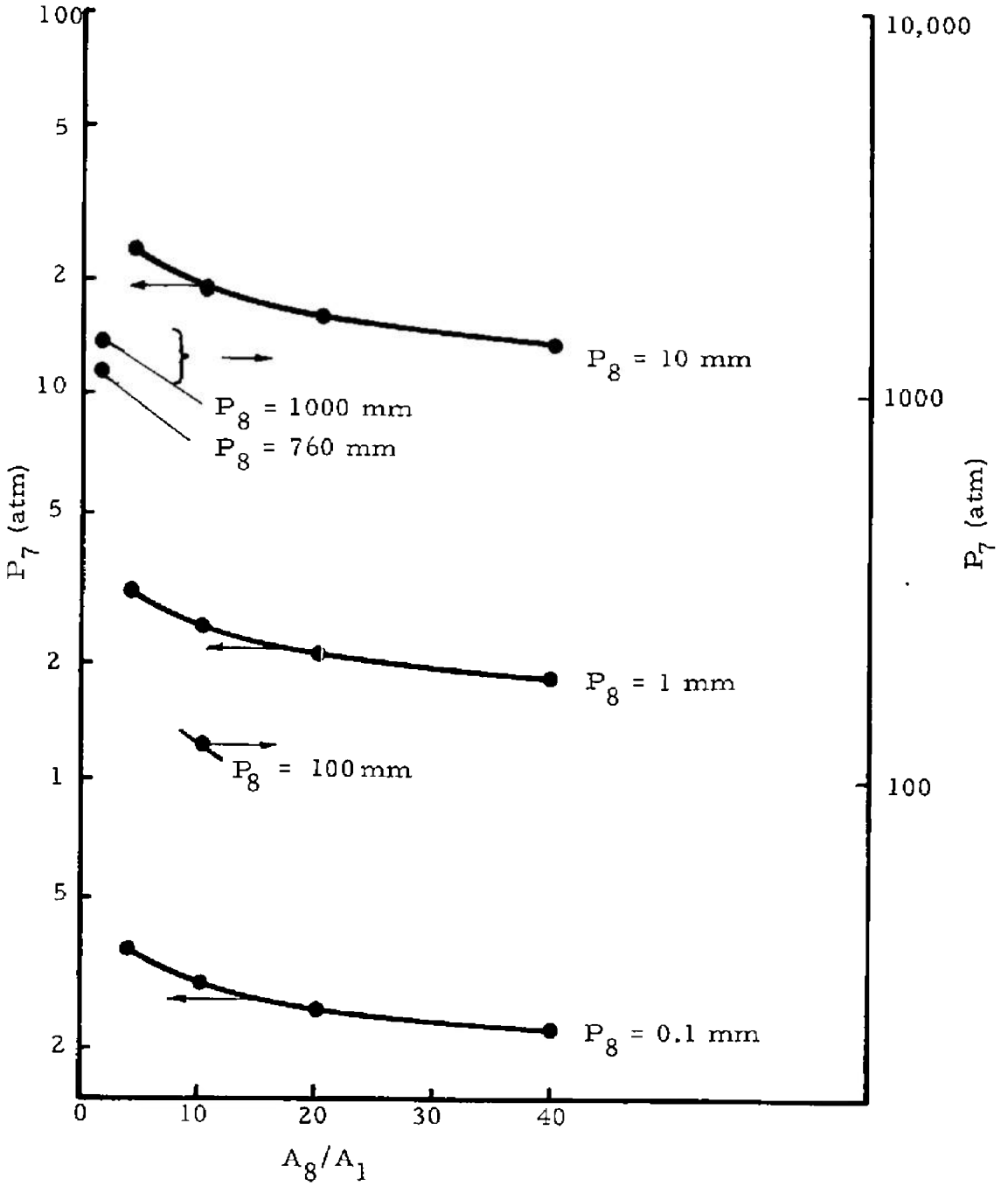

Fig. 5 Pressure Produced in Air for Various Shock Tube Test Parameters, 4000-atm Explosive Driver (Air data from Ref. 3)

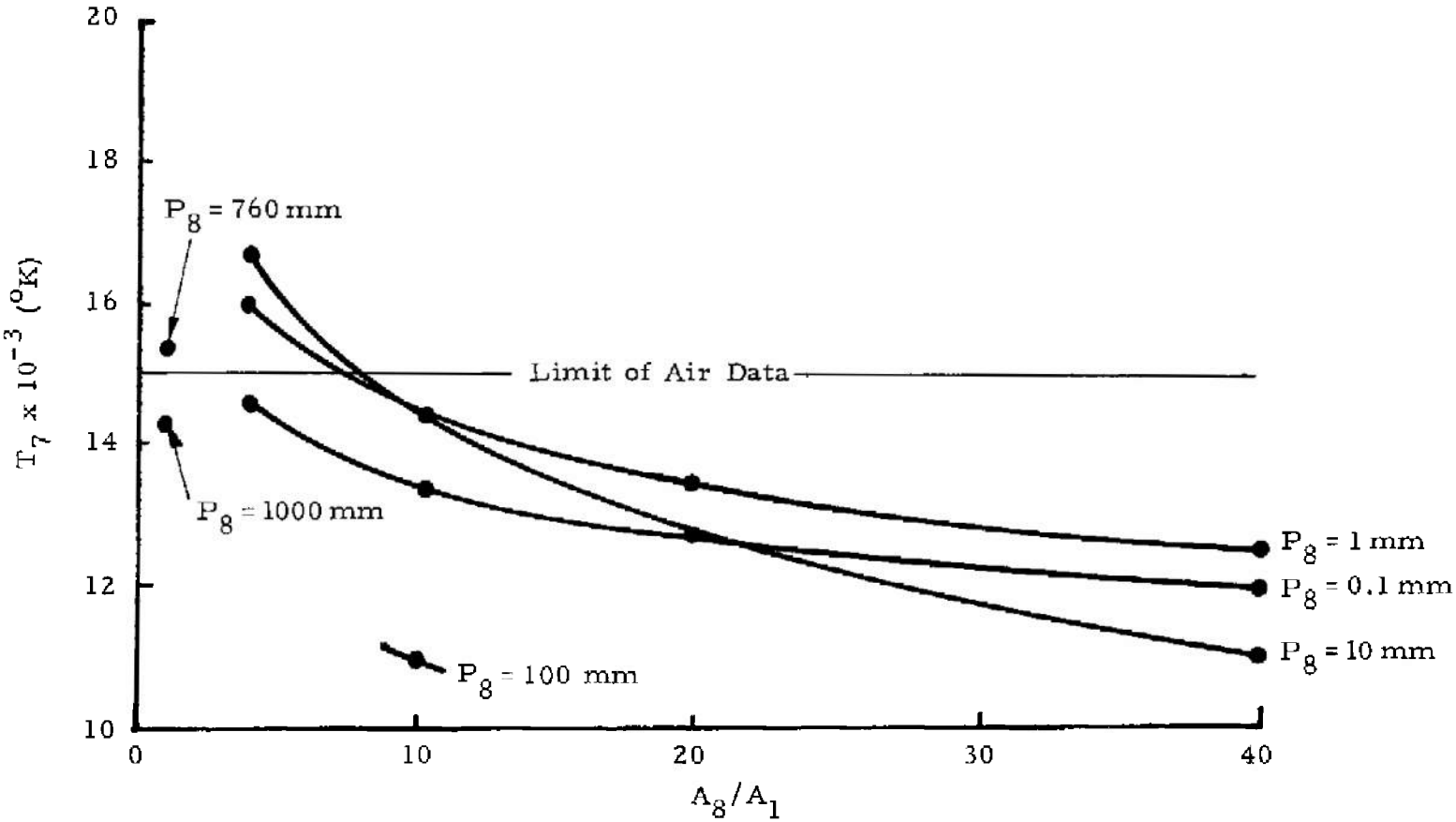

Fig. 6 Temperature Produced in Air for Various Shock Tube Parameters, 4000-atm Explosive Driver (Air data from Ref. 3)

in the test gas behind the shock wave, and the temperature T_7 in the test gas behind the shock wave are shown as functions of the area ratio A_8/A_1 between the driven section and the driver. These relations are given for various initial pressures P_8 in the driven section. Figure 6 shows that for an area ratio of approximately 10 between the driver and driven sections, the shocked gas temperature remains within the limits of the Hilsenrath and Klein description of air (15,000°K) for the pressure range from 0.1 to 100 mm Hg. Consequently, this ratio was incorporated into the design of the shock tube.

In an explosively driven shock tube, the termination of the explosive around the pressure tube brings the conical-shaped piston to an abrupt stop. This change in motion produces a rarefaction wave traveling downstream. The wave ultimately overtakes the contact front and destroys the uniform flow behind the incident shock. An expression is derived in the appendix that can be used to predict the length of shock tube traveled by the contact surface before it is overtaken by the rarefaction. This expression yields a value of 3 for the driven-to-driver-length ratio. On the basis of this analysis, the driven-driver-length ratio of the initial experiments was chosen to be 1.15 to avoid any possibility that the rarefaction would overtake the test gas.

C. PHYSICAL DESCRIPTION OF THE EXPLOSIVELY DRIVEN SHOCK TUBE

1. The Explosive Driver

A drawing of the complete shock tube is shown in Figure 7. The pressure tube used in the driver is a commercially available seamless steel tube 42 in. in length, with a wall thickness of 0.0625 in. and an internal diameter of 1.5 in. A soldered steel plug seals the upstream end of this tube, while a 0.022-in. polyester film diaphragm separates the driver from the driven section. The driver gas is helium that is initially at a pressure of 645 psi. The high explosive is contained by an acrylic tube with an internal diameter of 2.75 in. and a wall thickness of 0.125 in.

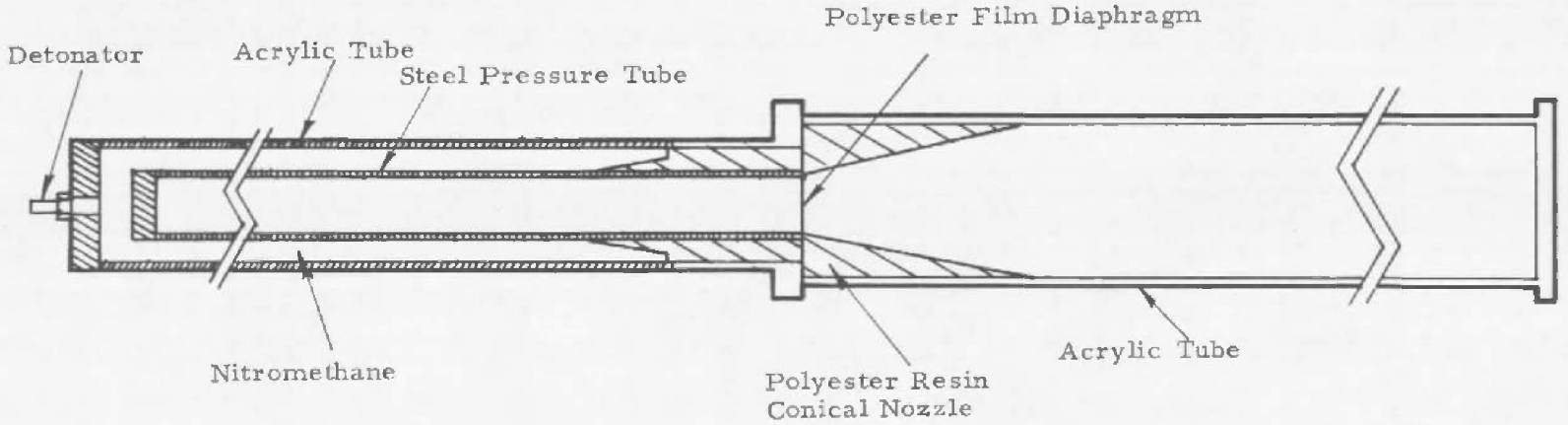

Fig. 7 Schematic Diagram of Complete Explosively Driven Shock Tube

Since the use of high explosives in the driver implies its destruction with every test, the economics of using it to drive a shock tube are of interest. The material cost (without diagnostics) of an explosive driver is roughly $70. Its weight is less than 30 lb. It contains 6.2 lb of nitromethane, which costs 35 cents per pound. The handling of nitromethane is simplified by the fact that the Interstate Commerce Commission classifies it as a commercial solvent.

2. The Driven Section

The driven section is an acrylic tube, 4.75 in. in internal diameter, with a wall thickness of 0.25 in. The acrylic tube was chosen for two reasons--(1) it permits continuous observation of the formation and propagation of the shock wave and gas column, and (2) it is an inexpensive, expendable shock tube. With the exception of one 13-ft driven section, the standard length was 4 ft.

A machined polyester resin nozzle is used to provide the steady expansion between the driver and the driven section. The nozzles used were conical-shaped with either a 15-deg or 30-deg total included angle.

A photograph of a complete shock tube assembly is shown in Figure 8.

D. BASIC INSTRUMENTATION

1. The Explosive Driver

The trajectories of the shock wave and detonation wave were determined primarily by means of shorting pins and piezoelectric transducers. The shorting pins are coaxial conductors whose conducting surfaces are separated by a small gap. They were placed through the nitromethane explosive and onto the pressure tube in precisely known positions. The gap is closed by the arrival of the shock wave, which short circuits an RC circuit and discharges through a raster-type oscilloscope. The time of arrival at the various predetermined positions then documents the trajectory of the shock wave.

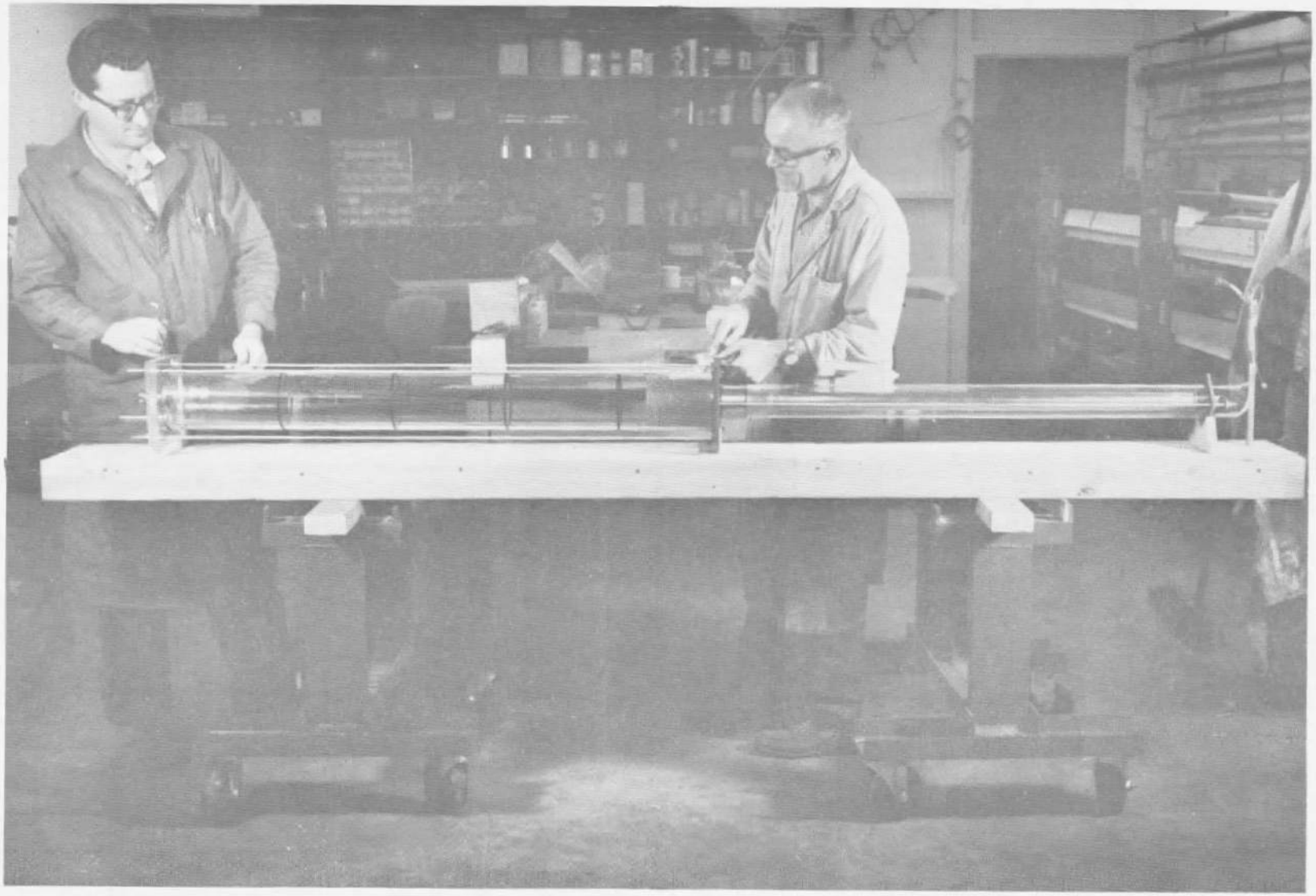

Fig. 8 Explosive Shock Tube Assembly

The piezoelectric transducers were used as time-of-arrival indicators to monitor the shock wave as well as the detonation front. Once the transit times of the shock wave through the nitromethane and container were determined, these units were precisely placed on the outside of the driver. As the shock wave traverses the barium titanate crystal used in the transducer, a voltage is produced across an external load. This voltage is proportional to the stress difference across the crystal. The pressures involved in the shock wave are sufficiently low to allow the transducer to respond again when the detonation wave passes. The outputs of the transducers were monitored by fast oscilloscopes. The time of arrival at known positions permits the trajectories of the shock wave and detonation wave to be determined by the same instrumentation.

A pulsed X-ray system was used to record the implosion of the pressure tube and the formation of the conical-shaped piston. A Marx-type generator, designed and built by Physics International, drives a remotely located Fexitron Model 506A X-ray tube. The generator is capable of operating between 300 and 600 keV and produces a 0.2-μsec burst of X-rays by the passage of 1 kA through the tube. To produce an image, Royal Blue X-ray Film was used in conjunction with DuPont Patterson Industrial Combination X-ray intensifying screens. Since the film and screens are subject to severe blast exposure, they were protected by aluminum cassettes that prevent film damage. Figure 9 shows a typical radiograph of the imploding pressure tube. The conical-shaped piston of the explosive driver is shown at the time the detonation wave reaches the end of the explosive.

2. The Driven Section

Since the velocity of the shock wave is probably the most useful parameter used to describe the performance of a shock tube, several different techniques were used to determine the shock velocities produced in the explosively driven shock tube.

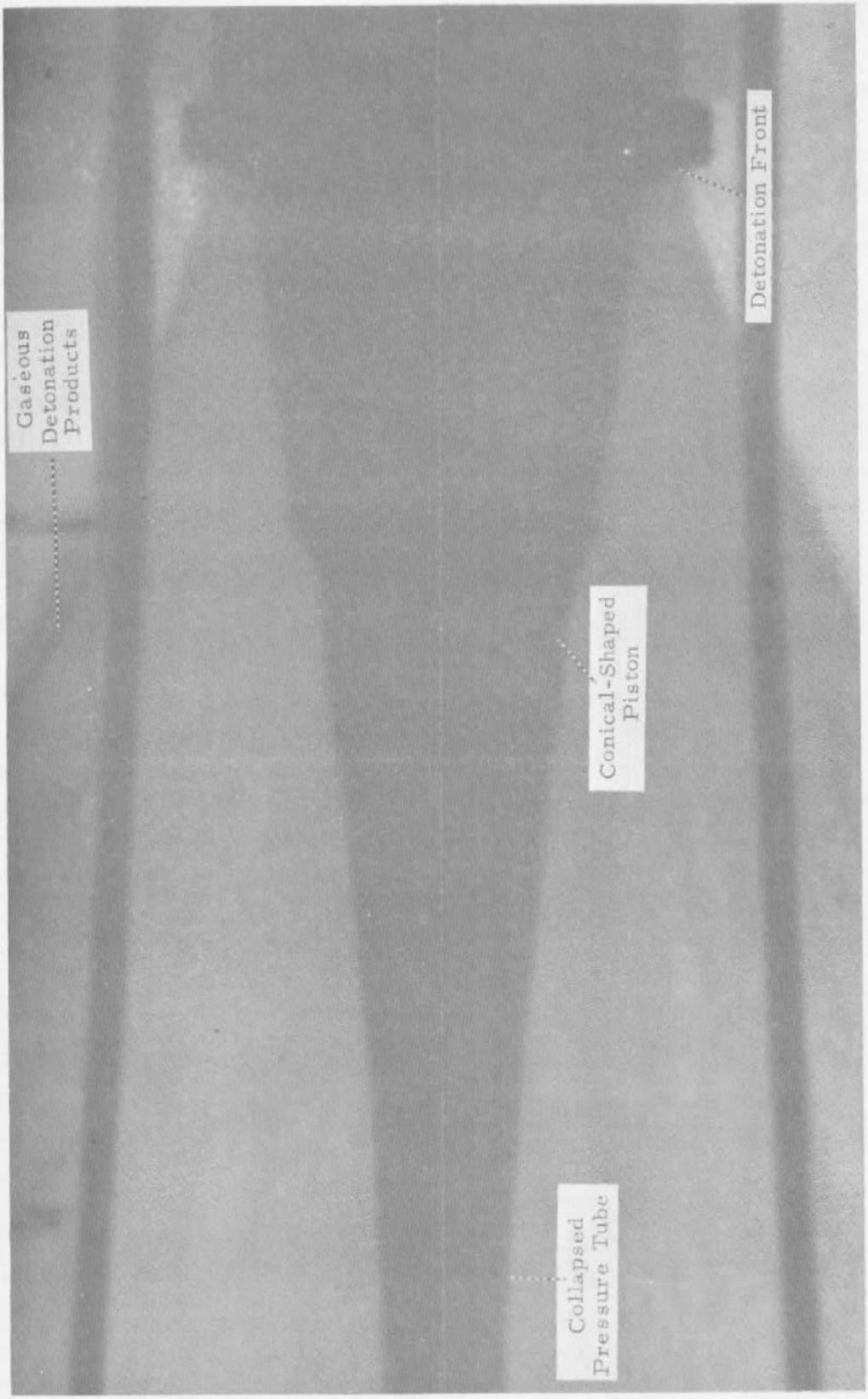

Fig. 9 Radiograph of Collapsing Pressure Tube of an Explosive Driver

The most accurate and descriptive technique was the use of a high-speed framing camera to record the motion of the highly luminous shock wave. In addition, the extreme difference in the intensity of light emitted from the helium driver gas makes it possible to observe the helium-air interface that is assumed to be the contact surface. As a result, this technique documents the entire formation and growth of the shocked air sample. Several examples of the type of information obtained by this technique are shown in the next section. (It should be noted that these are black-and-white reproductions of a high-speed Ektachrome film strip, and much of the detail has been lost in the process.) Neutral-density filters were used on alternate frames of the camera to look for detailed structure (e.g., turbulence and viscous effects) within the extremely luminous shocked air sample. In addition, Edgerton, Germeshausen, and Grier's extended-range film was often used to observe detail under the widely ranging light conditions (Ref. 4). This film consists of three emulsions and has a usable exposure latitude of 10^8 in the visible region of the spectrum.

Phototransistors (14A643) having a rise time less than or equal to 25 nsec were operated as diodes to monitor the luminous front of the shock wave. A number of these were collimated and precisely positioned perpendicular to the flow. Figure 10 is an oscilloscope record showing the response of two of these diodes. The lower trace of this figure is the output of two diodes that have been added algebraically using Type CA Tektronix Dual Trace Amplifiers. The outputs of the diodes indicate the time of arrival at their respective positions. From this information, the average velocity between positions can be determined. In addition, the duration of the diode output is related to the test time of the gas.

Several experiments used a resistive wire gauge to provide a continuous history of the shock velocity. A high-resistance bare wire is secured along the inside wall of the shock tube parallel to the axis. A low-resistance wire is placed alongside the high-resistance wire and soldered on the upstream end to form a tight loop. A constant

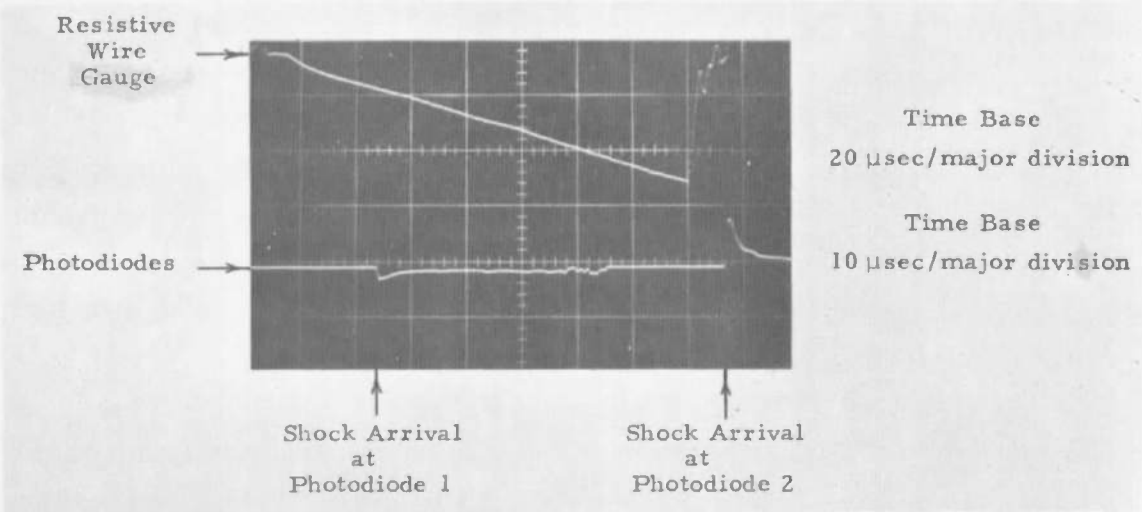

Fig. 10 Examples of Data Generated by Photodiode and Resistive Wire Instrumentation

current is passed through this loop and the resulting voltage drop displayed on an oscilloscope. As the shock front passes over this loop, it progressively short circuits part of the loop and continually changes the voltage being monitored. The rate of voltage change is directly proportional to the velocity of the shock wave. A typical response is shown in the upper trace of Figure 10.

The other methods that have been used for determining shock velocities--ionization pins and piezoelectric transducers-- are standard techniques that have been detailed by various authors (Refs. 5, 6) and will not be repeated here.

A measurement of shock velocity and gas velocity insures, through the conservation of momentum, a knowledge of the pressure behind a shock wave. However, a piezoelectric pressure transducer was mounted in the downstream end plate to monitor the reflected shock pressure and compare it with the value predicted by assuming the gas is described by the same ratio of specific heats after the reflection as before. Figure 11 shows a typical signal. Thermocouple gauges, mercury manometers, and Wallace and Tiernan absolute pressure indicators were used in their appropriate pressure range to determine the initial pressure in the test section.

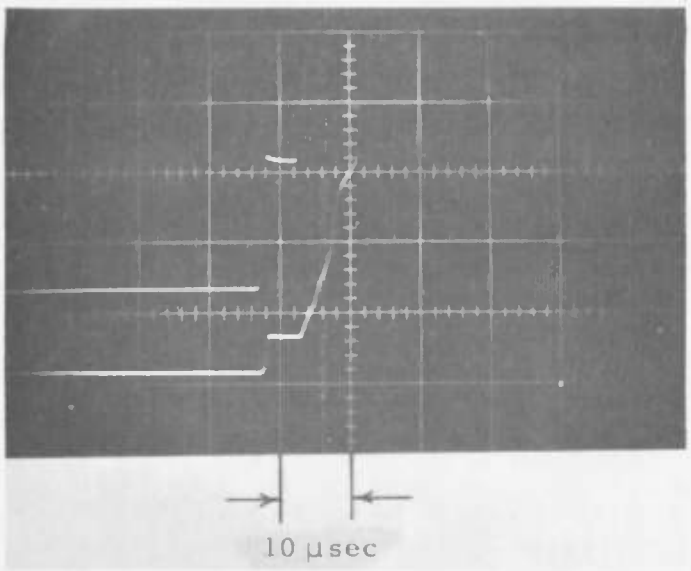

Fig. 11 Response of Pressure Transducer Placed on Axis at the End of Driven Section of Shot ST-5

SECTION III
EXPERIMENTAL RESULTS

A total of nine experiments were conducted to investigate the feasibility of using an explosive driver to drive a shock tube. The results of these experiments are summarized in Table II. Here the observed shock velocity, gas velocity, and the gas pressure derived from these velocities are compared with their predicted values for the test parameters studies. The symbols and nomenclature used are consistent with the wave diagram shown in Figure 3 with the exceptions of θ, which is the total included angle of the nozzle, and τ, which is the testing time at a position of $x/L_1 = 1$. The experimental firings (shots) have been grouped according to the initial pressure of air in the test section. All firings utilized a 4000-atm driver except Shot ST-2, which used a 2000-atm driver (Section III F). A more graphic summary of some of these data is given in Figure 12. This figure presents the observed and predicted shock velocities for various initial test gas pressures P_8 and area ratios A_8/A_1. The details of the individual experiments (shots) are discussed in the sections that follow. For purposes of comparison, a summary is given of the performances of shock tubes using various different driver techniques.

A. SHOTS AT INITIAL PRESSURE OF 10 mm, 4000-atm DRIVER

Shot ST-1

This was the first experiment utilizing the explosive driver. The area ratio $A_8/A_1 = 10$ and the length ratio $L_8/L_1 = 1.15$ were chosen from the theoretical considerations discussed previously. A 30-deg conical nozzle provided the steady expansion between the driver and driven sections.

The results of this shot are shown in the wave diagram of Figure 13. The agreement between the observed shock velocity of 38,550 ft/sec and the predicted value of 37,590 is quite good. Detailed structure of the shocked gas was not visible in the color film of the

TABLE II
SUMMARY OF PERFORMANCE OF EXPLOSIVELY DRIVEN SHOCK TUBES

Shot No.	Test Parameters				Theoretical Predictions						Experimental Results				Comments
	A_2/A_1	L_2/L_1	θ (deg)	P_6 (mm Hg)	Shock Velocity U_{s8} (ft/sec)	Gas Velocity U_7 (ft/sec)	Pressure P_7 (atm)	Temperature T_7 (°K)	Density ρ_7 (amagats)	Test Time at $x/L_1 = 1$ (μsec)	Shock Velocity U_{s8} (ft/sec)	Gas Velocity U_7 (ft/sec)	Pressure P_7 (atm)	Test Time at $x/L_1 = 1$ (μsec)	
4000 ATMOSPHERE DRIVER															
ST-1	10	1.15	30	10	37,589	34,839	18 945	14,381	0 1633	7.66	38,550	35,430	21.5	<13	First experiment, good agreement with theory
ST-3		1 15	30								38,620	35,170	21 4	7 5	Shot identical to ST-1, good reproducibility
ST-5		1.15	15								39,760	38,710, 35,760	24.3	4-12	Change of nozzle angle seems to effect flow properties
ST-6		3.79	15								38,710+ 36,420	37,070+ 35,110	22 6- 20.2	10	Gas flow properties change at $x/L_1 \approx 2$
ST-4		1.15	30	0.1	46,589	43,947	0.2959	13,355	0.0081	4 67	58,400	--	--	--	Shock front unstable and considerably faster than predicted
ST-7		1.15	15	100	29,829	27,626	119,2	11,004	1.6184	9.72	30,000	28,410	134	8	Excellent agreement with theory
ST-8	1	1.15	0	1000	32,180	29,465	1371 6	14,282	14.203	10 46	30,510+ 21,000	26,580+ 21,000	1280- 695	13	Radial expansion of shock tube section decelerates shock front.
ST-9	10	1.15	30	1	43,007	40,213	2.5	14,438	0.01835	5.87	46,910	44,290	3.28	5,6	Shock front stable, reasonably uniform shocked gas column, shock velocity higher than predicted
2000 ATMOSPHERE DRIVER															
ST-2	10	1 20	30	10	--	--	--	--	--	--	35,600	34,600	19 43	7 5	Driver did not function as directed

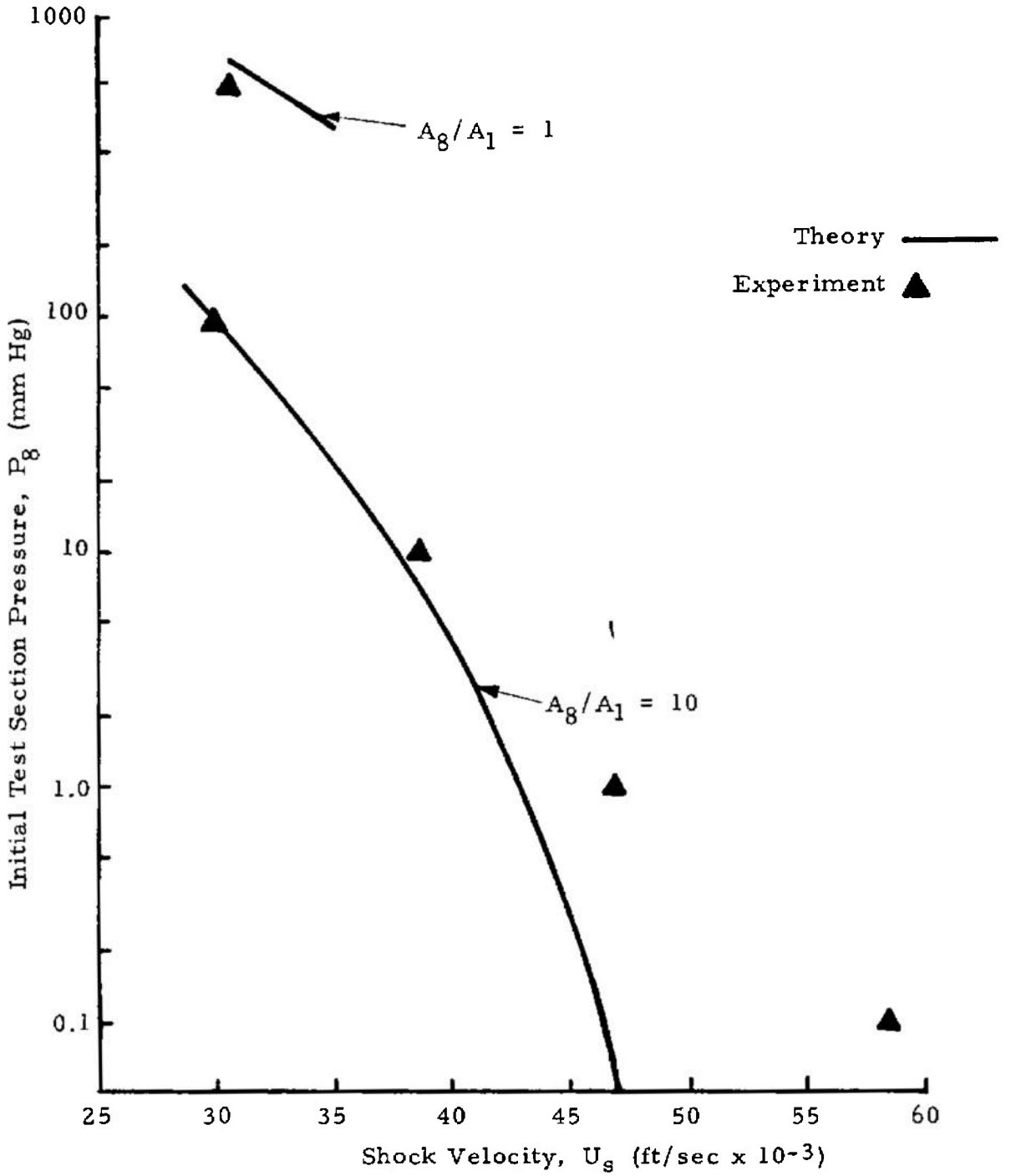

Fig. 12 Predicted and Observed Performance of a Shock Tube Using a 4000-atm Explosive Driver

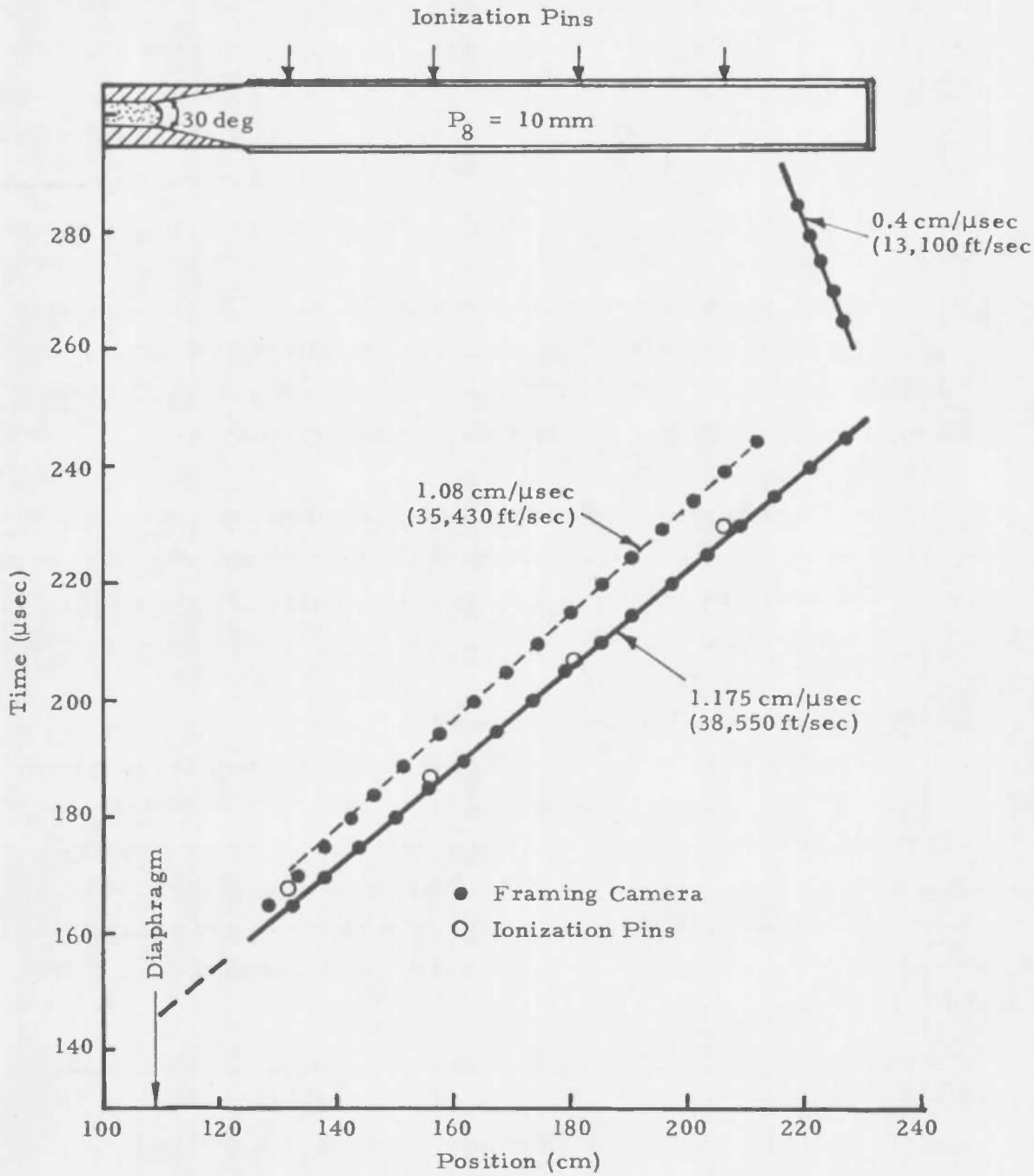

Fig. 13 Experimental Results of Shot ST-1

framing-camera record. The high-intensity light emitted from this region caused local overexposure of the film in spite of an effective aperture of F/21 and an exposure time of 0.9 μsec. The overexposure caused halation (light scatter) in the color film emulsion. The apparent interfaces produced by this effect were originally interpreted as the actual shock front and contact surface boundaries. As a result the observ· length of shocked gas, and therefore test time, was much too large.

Shot ST-3

This experiment was identical to Shot ST-1. The primary purpose of this shot was to determine the reproducibility of the explosively driven shock tube. In addition, a repeat shot provided the opportunity to concentrate on diagnostic and instrumentation techniques.

The observed velocities of the shock wave and contact surface were 38,620 ft/sec and 35,170 ft/sec, respectively. These values were in excellent agreement with the corresponding values, 38,550 ft/sec and 35,430 ft/sec, of Shot ST-1.

Neutral-density filters were used to prevent halation in the color film. As a result more details were visible in the area of the shocked gas. For example, the planar shock front was followed by a disc-shaped region of uniform luminosity, and then a cup-shaped area of varied luminosity that faded in time. For measurements of contact surface velocity and test time, only the disc-shaped region was considered to be the shocked test gas. A sequence of the framing-camera record of this shot is shown in Figure 14.

Shot ST-5

The only test parameter changed for this shot was the angle of the nozzle providing the transition between the driver and driven sections. The nozzle for this shot had a total angle of 15 deg. The object was to determine the effect of the steady expansion produced by the nozzle on the dynamics in the shock tube.

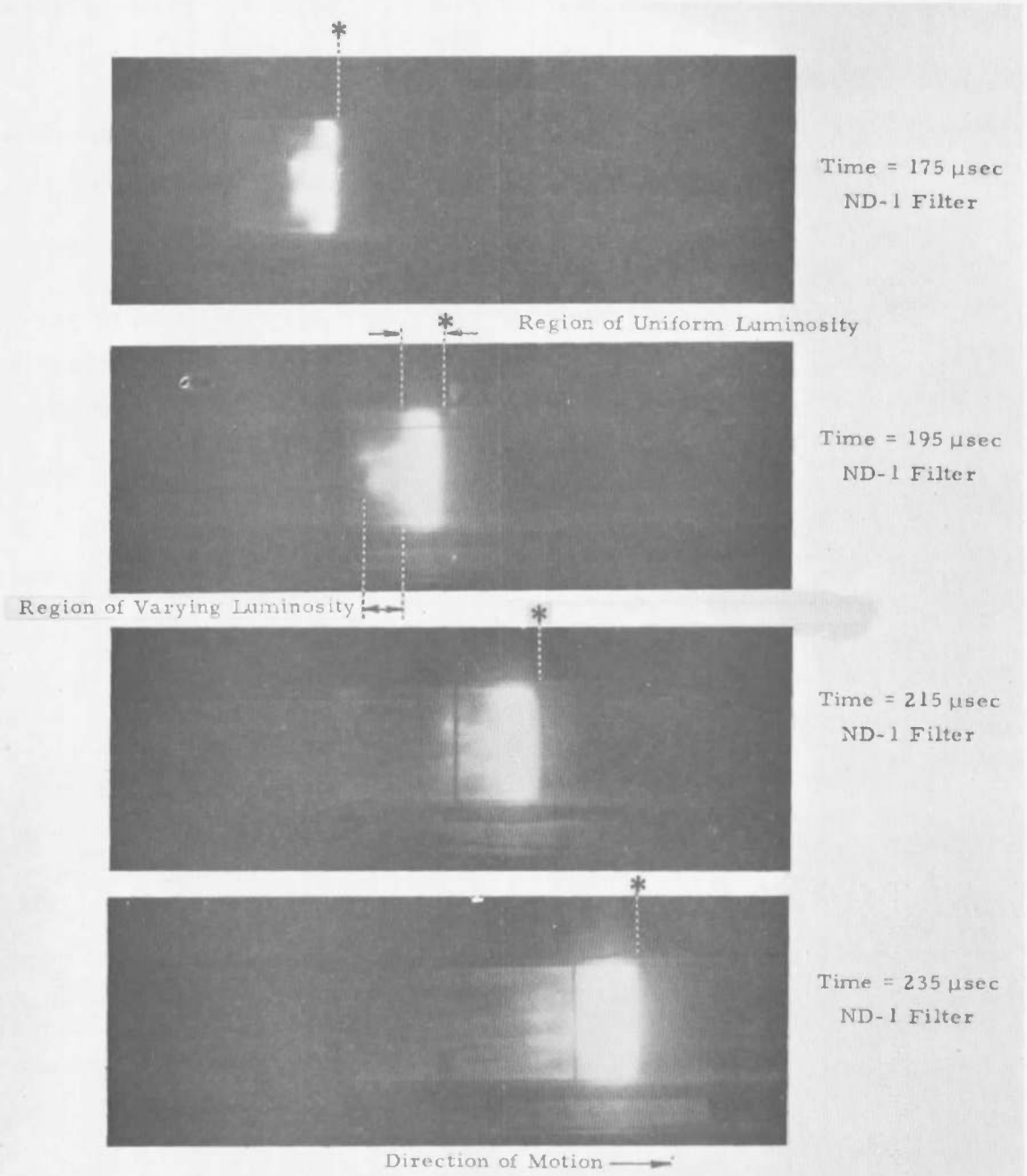

Fig. 14 Block and White Reproductions of Color Froming Comera Sequence of Shot ST-3 (Asterisk indicotes shock front)

The shock velocity was found to be 39,760 ft/sec, approximately 3 per cent above that of Shot ST-1. The shocked gas appeared to be separating into two parts shaped somewhat like an hourglass. The film sequence in Figure 15 shows this shape during its transit of the shock tube. The front portion of this shape has a velocity of 38,710 ft/sec, while the velocity of the rear section is approximately 35,760 ft/sec. From the reproducible performance established by Shots ST-1 and ST-3, it was concluded that the higher shock velocity and hourglass appearance were related to the expansion of the gas through the 15-deg nozzle.

Shot ST-6

The purpose of this shot was to assess the effect on shock-tube performance of a driven section that is long compared to the driver length. The length ratio of the shock tube was increased from the previously used L_8/L_1 of 1.15 to a value of L_8/L_1 equal to 3.79.

The results of this shot are illustrated in the wave diagram of Figure 16. An initial shock velocity of 38,710 ft/sec and interface velocity of 37,070 ft/sec were recorded by a framing camera and phototransistors. After a length of x/L_1 equal to approximately 2.16, a change of velocities occurs in which the shock velocity is recorded as 36,420 ft/sec and the interface velocity as 35,110 ft/sec. There was no observable change in the light intensity emitted from the shocked gas during its entire transit of the driven section. Since the first rarefaction wave produced by the stopping of piston was predicted to overtake the contact front at x/L_1 equal to approximately 3 (see Appendix), it appears that other phenomena such as viscous effects are contributing to the change in velocity.

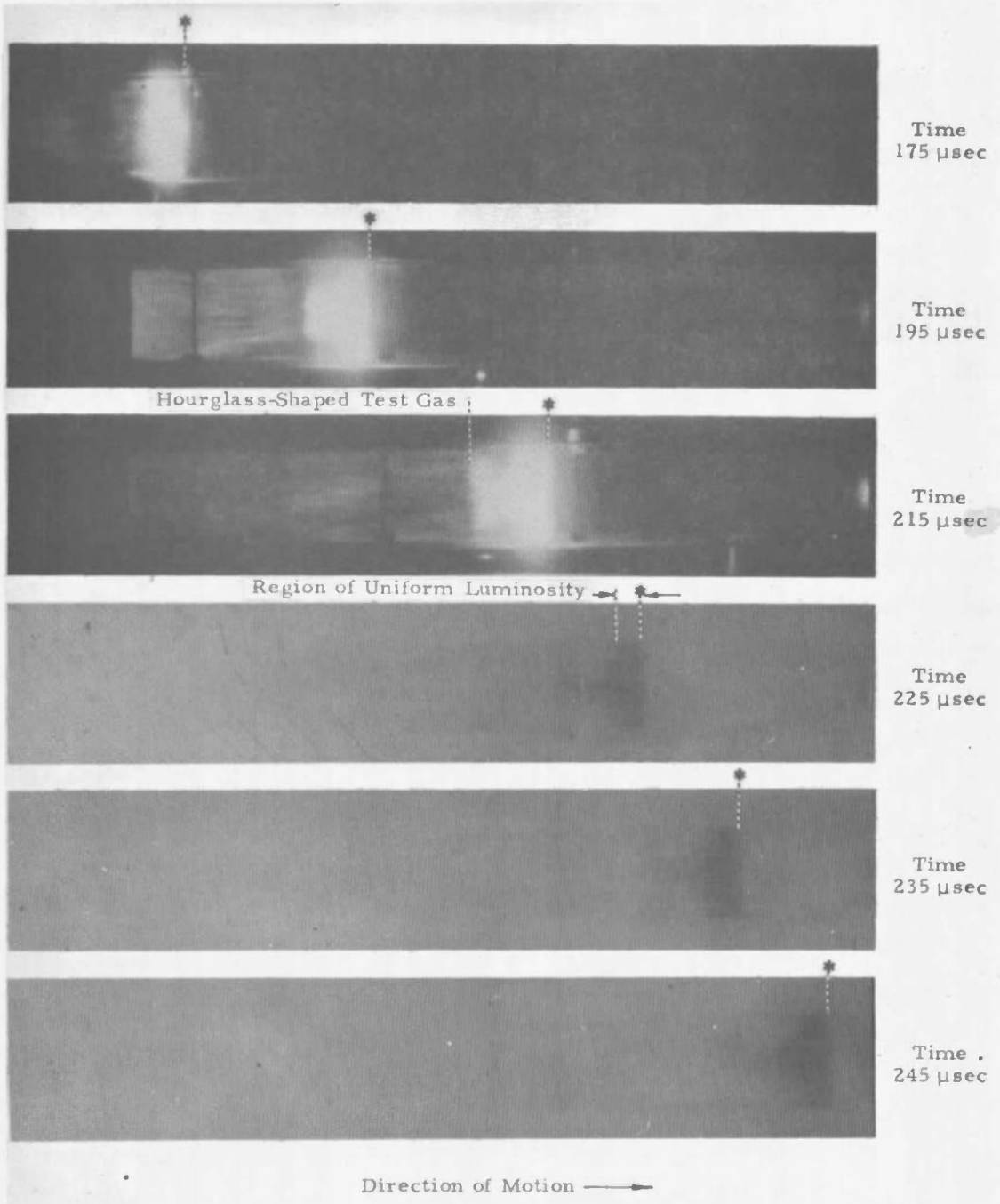

Fig. 15 Block and White Reproductions of Color Froming Comero Sequence of Shot ST-5 (Top three photographs high-speed Ektachrome film, lower three EG&G extended-ronge film) (Asterisk indicotes shock front)

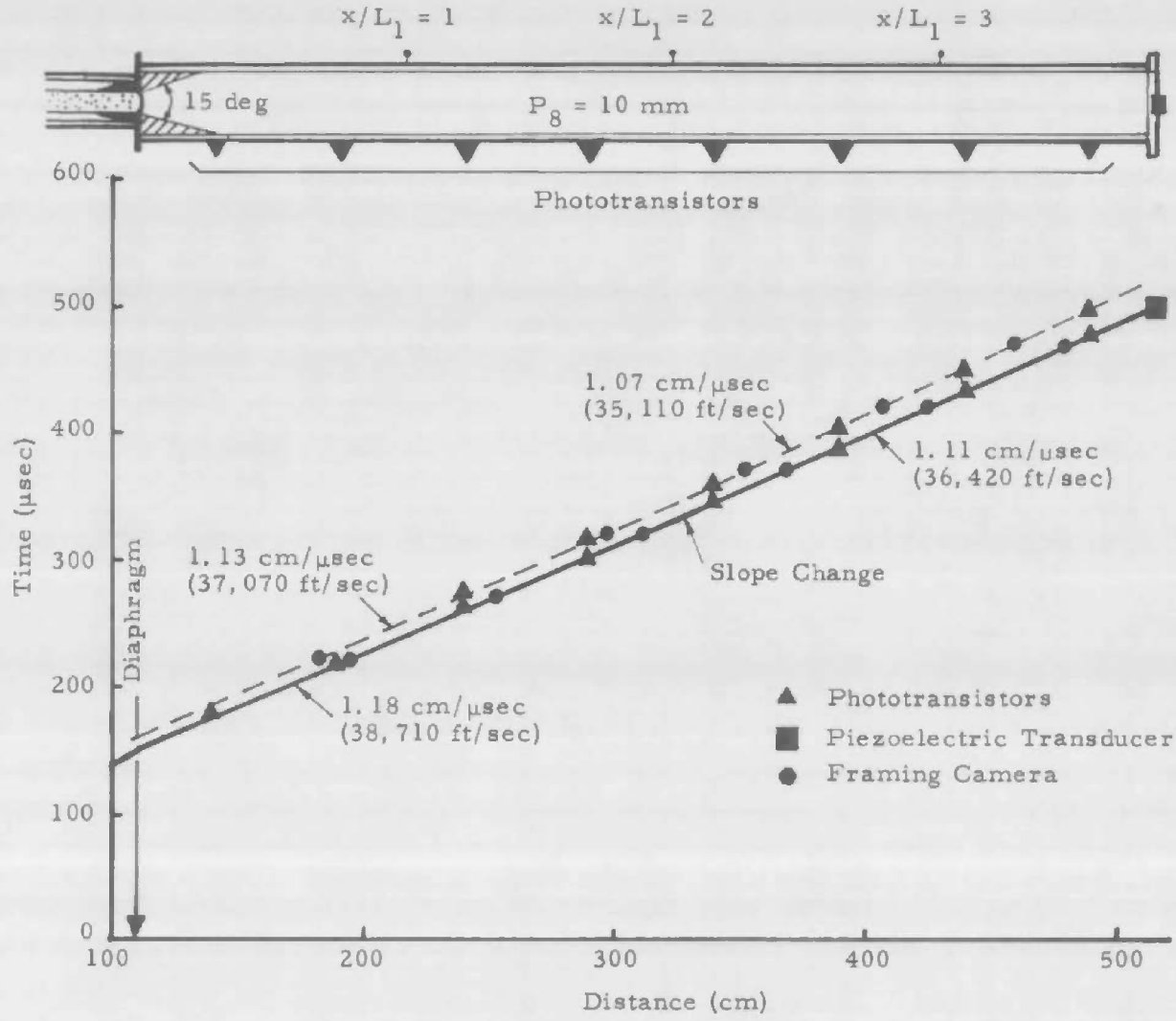

Fig. 16 Experimental Results of Shot ST-6

B. SHOTS AT INITIAL PRESSURE OF 0.1 mm, 4000-atm DRIVER

Shot ST-4

This was the first of a series of shots in which the initial pressure P_8 in the test section was varied. A film sequence of this shot is shown in Figure 17. A luminous cylindrical shape is seen emerging from the nozzle (t = 172.5 μsec); it soon fills the inside diameter of the shock tube, forming a rather luminous shock front. The velocity of the shock front is constant and equal to 58,400 ft/sec. This is considerably higher than the predicted value of 46,589 ft/sec. The orientation of the shock front varied in time, giving the appearance of being unstable. Also, the luminosity of the shocked gas was quite low, making a gas-velocity measurement meaningless. It is possible that the unusual rod-like shape on the axis as well as the higher shock velocity was a result of the coalescence of waves after the gas emerged from the nozzle.

C. SHOTS AT INITIAL PRESSURE OF 100 mm, 4000-atm DRIVER

Shot ST-7

The experimental results of this shot are shown in the wave diagram of Figure 18 and the framing camera sequence of Figure 19. The observed shock velocity of 30,020 ft/sec was in excellent agreement with the predicted value of 29,829 ft/sec. The luminous interface between the test and driving gas had a velocity of 28,410 ft/sec compared to the predicted value of 27,626 ft/sec. The rectangular-shaped luminosity at t = 255 μsec of Figure 19 is the light emitted from an explosively driven argon light source used to attempt to see more detail in the shocked gas region by photographing it in a shadowgraph arrangement. As shown by this frame, the light emitted from the shocked test gas made it opaque to the argon light source.

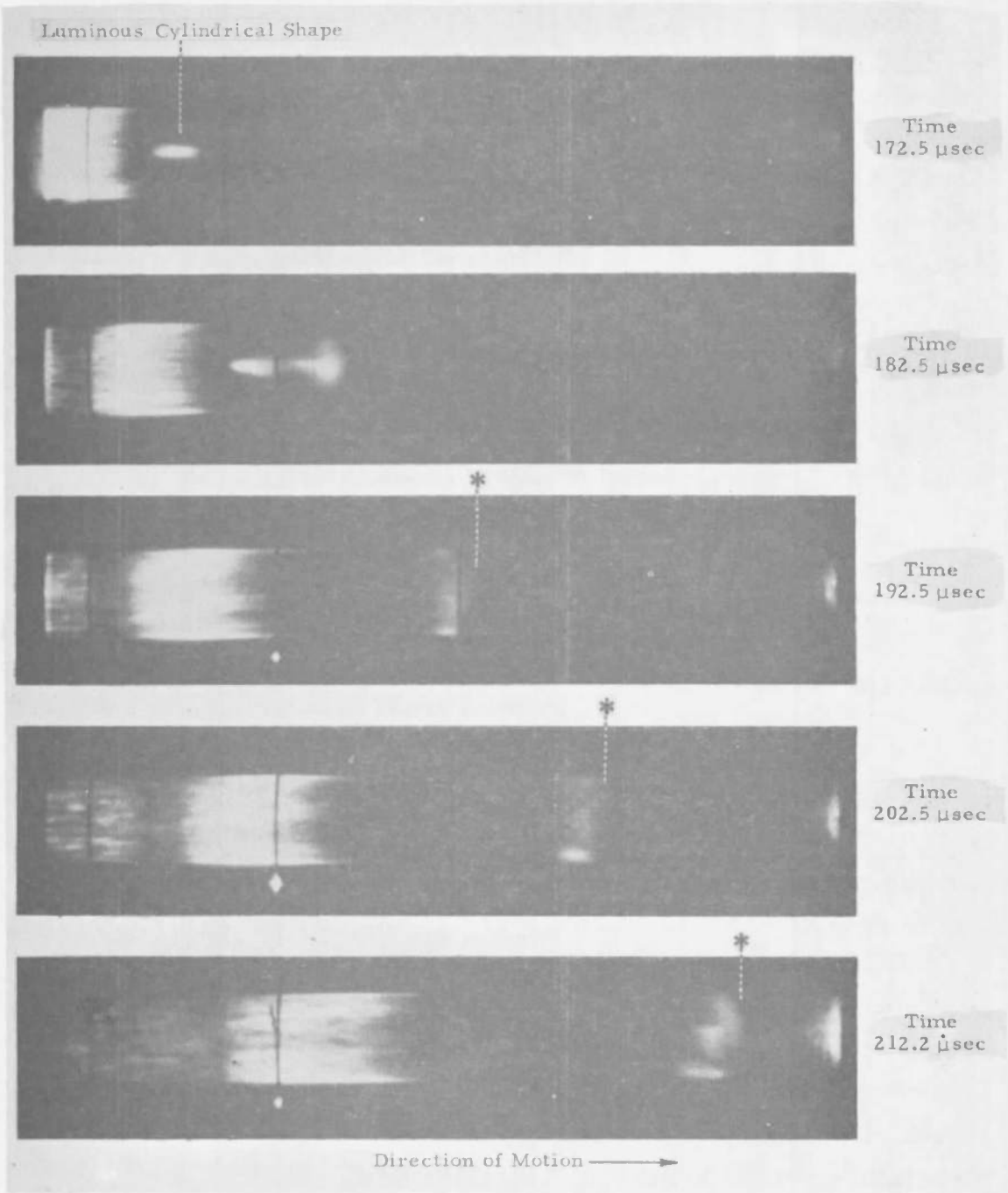

Fig. 17 Block and White Reproductions of Color Froming Camera Sequence of Shot ST-4 (Asterisk indicates shock front, appears unstable)

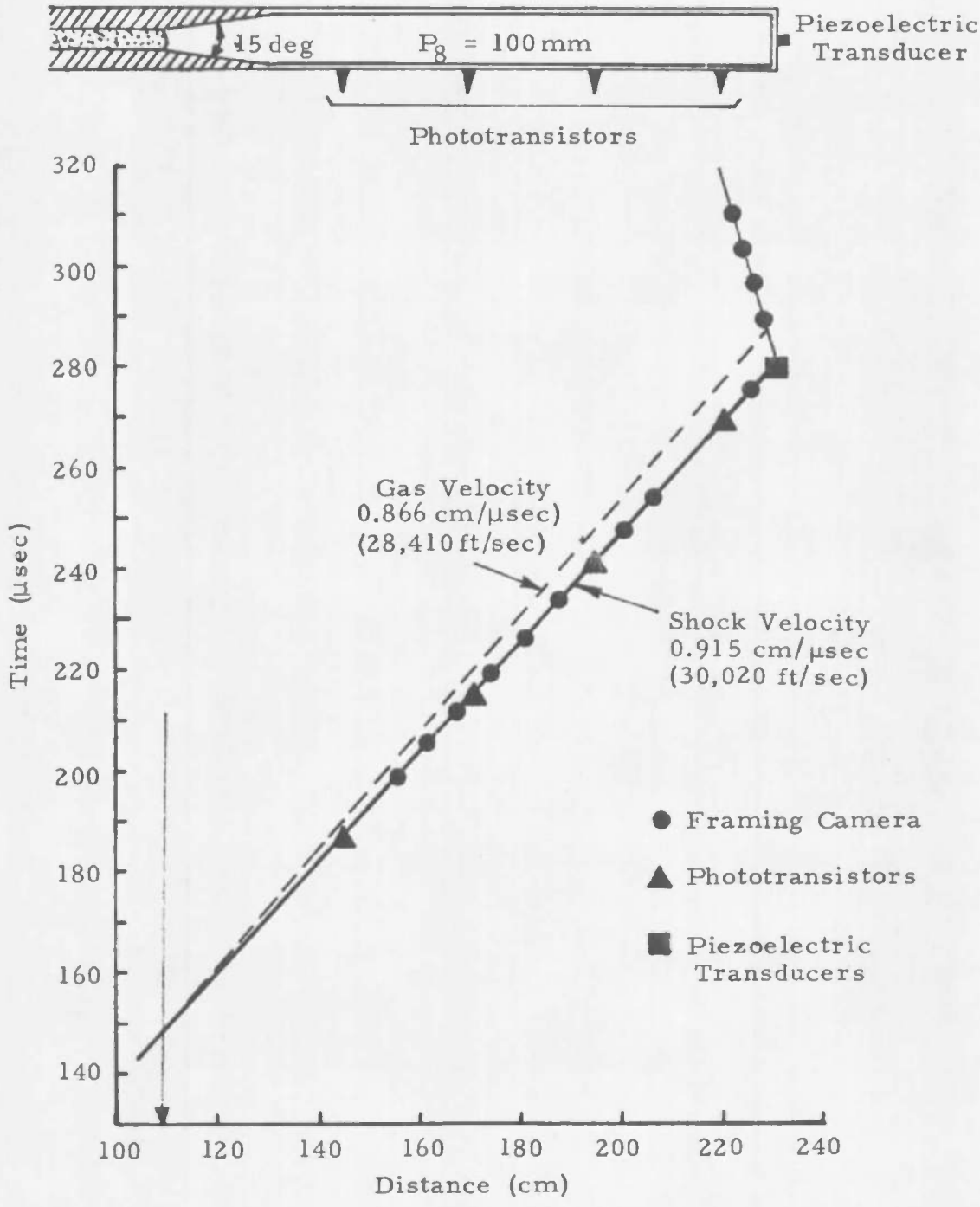

Fig. 18 Experimental Results of Shot ST-7

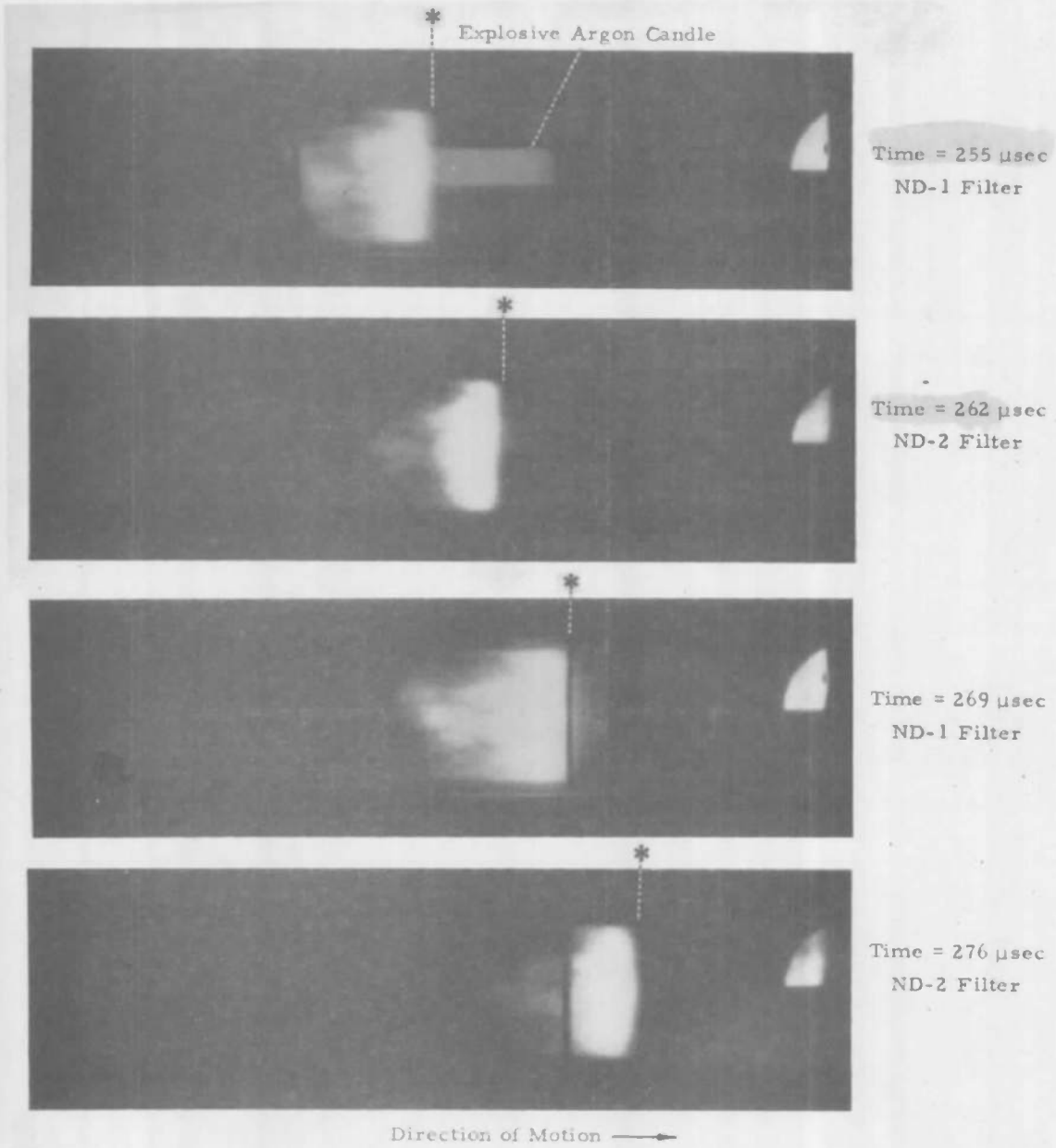

Fig. 19 Block and White Reproductions of Color Froming Camera Sequence of Shot ST-7 (Asterisk indicates shock front)

D. SHOTS AT INITIAL PRESSURE OF 1000 mm, 4000-atm DRIVER

Shot ST-8

The test parameters of this shot varied considerably from previous shots in that the area ratio A_8/A_1 was made equal to 1.0. The results of this shot are given in Figures 20 and 21. These results show that the shock wave emerged from the driver section with a velocity of 30,510 ft/sec compared to the theoretical value of 32,180 ft/sec. As the shock wave continued, however, it was found to decelerate rather slowly and uniformly to a velocity of 21,000 ft/sec near the end of the driven section. The length of the column of shocked test gas increased uniformly to about 8 cm at a point approximately halfway down the shock tube and remained at this length for the duration of its travel. The deceleration of the shock was due to the radial expansion of the acrylic shock tube, t = 208 μsec in Figure 21. Since the pressure behind the shock wave (P_7 = 1280 atm) exceeded the dynamic yield strength of the acrylic tube, the resulting rarefaction waves dropped the pressure behind the shock wave and decelerated the shock front. The probability of tube expansion had been realized prior to firing this shot. However, calculations showed there would be very little radial displacement during the time of interest, i.e. transit time of the shocked test gas.

E. SHOTS AT INITIAL PRESSURE OF 1 mm, 4000-atm DRIVER

Shot ST-9

Since the agreement between predicted and observed shock-tube performance was considerably better for the higher test gas pressures, it was speculated that the poor agreement at the pressure of 0.1 mm (Shot ST-4) might have resulted from some unobserved malfunction of the driver section. As a result, this experiment was conducted to re-evaluate the performance of the shock tube at rather low pressures. The shock velocity observed for this shot was 46,910 ft/sec. A luminous cylindrical shape similar to that observed in Shot ST-4 was seen emerging from the nozzle; however, it soon formed a well-defined shock front and

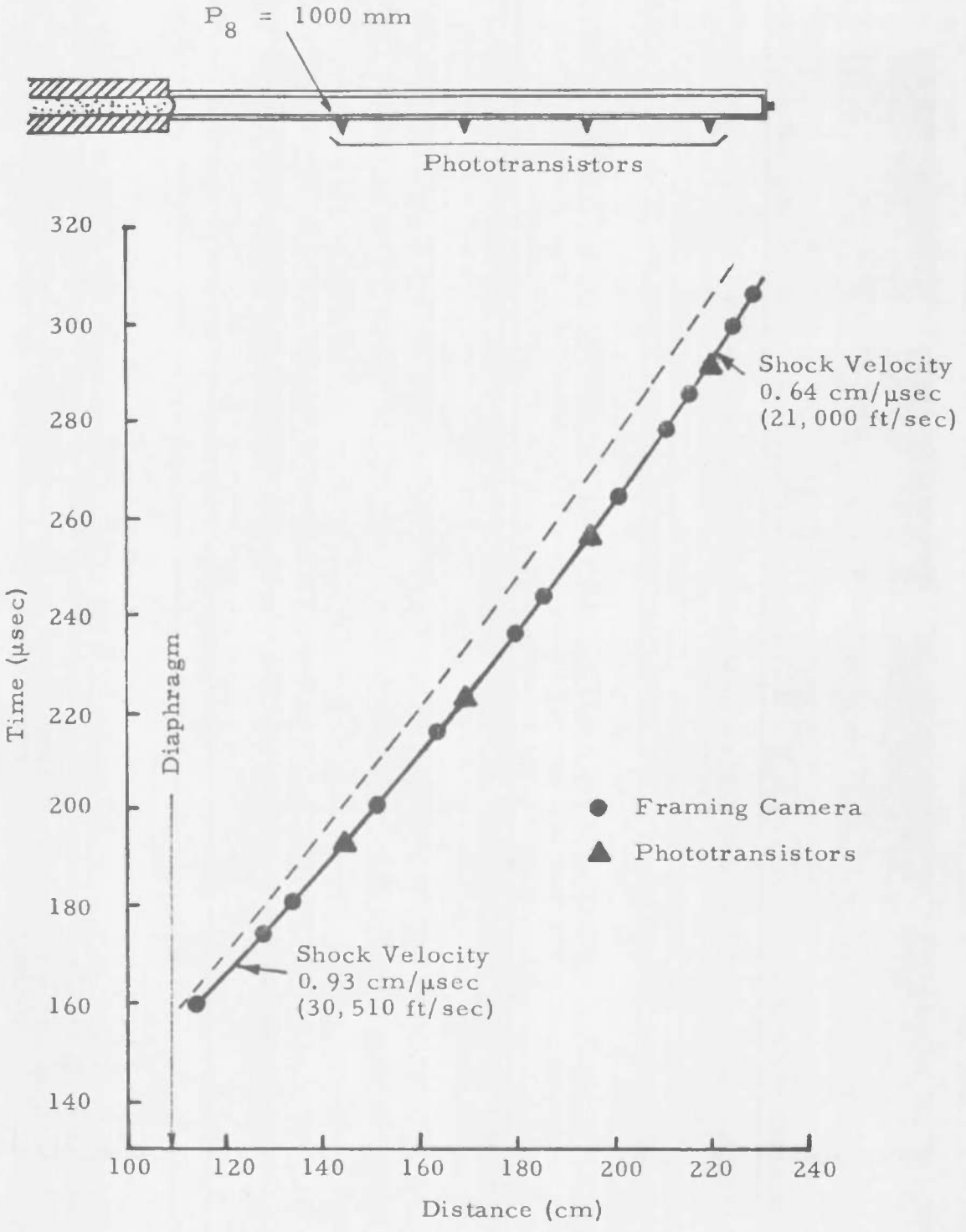

Fig. 20 Experimental Results of Shot ST-8

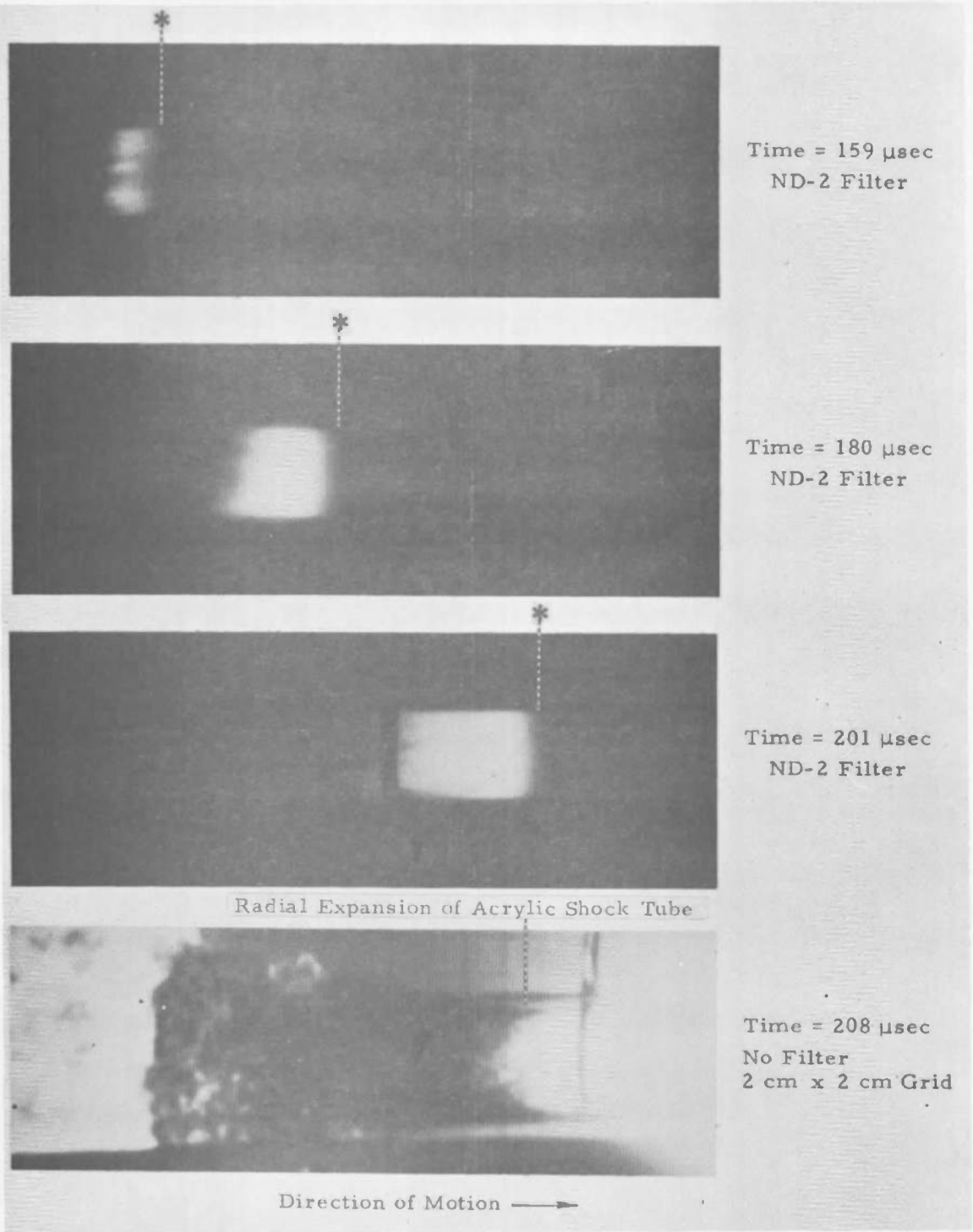

Fig. 21 Black and White Reproductions of Color Framing Camera Sequence of Shot ST-8 (Asterisk indicates shock front)

shocked-gas column. The gas was observed to have a velocity of 44,290 ft/sec. While the observed shock and gas velocities did not agree with their predicted values, they did confirm the trend of higher shock-wave and gas velocities at the lower pressures.

F. SHOTS AT INITIAL PRESSURE OF 10 mm, 2000-atm DRIVER

Shot ST-2

In the anticipation of eventually changing the operating regime of the standard driver, a single modified driver was designed to minimize the two-dimensional and non-steady conditions caused by the radial expansion of the pressure tube. The pressure tube used in this experiment, with an outside diameter of 9/16 in. and a 0.035-in. wall, contained helium at 323 psi. This loading pressure results in a 2000-atm shock wave for the nitromethane explosive system. A steel tube, 3.5 in. in outside diameter with a 0.75-in. wall, surrounded the nitromethane and served as an inertial tamper. Ideally, the tamper will not yield to the 2000-atm pressure of the initial shock wave; instead, the pressure tube will expand a small amount until an equilibrium position is reached. Now the conditions presented to the detonation wave are almost one-dimensional and constant in time.

The results of these shots indicate the driver did not function properly, Figure 22. The collapse of the pressure tube is believed to have produced a metal vapor or jet region that created a shock wave having a velocity considerably higher than the anticipated value of 28,100 ft/sec. This, however, did not prevent the formation of the shock wave in the driven section. The shock and gas velocities were recorded at 35,600 ft/sec and 34,600 ft/sec, respectively. This experiment emphasized the importance of experimentally verifying the operation of any extrapolations (e.g., geometry, size, operating regime) of the standard design.

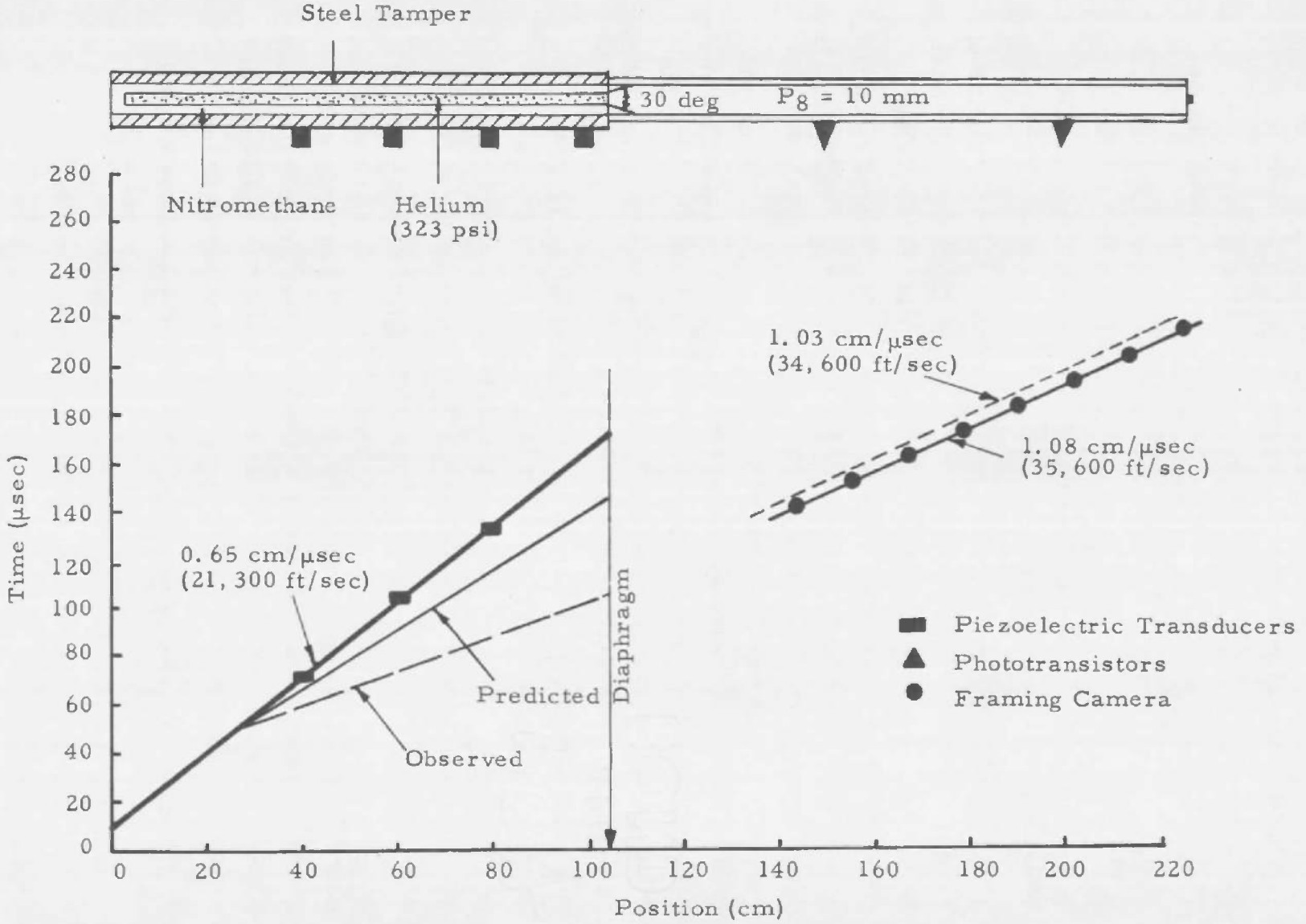

Fig. 22 Experimental Results of Shot ST-2 (2000-atm Driver)

G. COMPARISON OF DIFFERENT DRIVER TECHNIQUES

Figure 23, reconstructed from Reference 7, shows the theoretical performance of a particular air shock-tube design for various driver techniques. The drivers considered are: room-temperature hydrogen, the products of combustion of a hydrogen-oxygen mixture, and high-temperature helium drivers such as the ones currently being used in electrically heated shock tubes (Refs. 7, 8, 9). The predicted performance of these drivers is based on a driver pressure of 1000 atm (a practical value from a design standpoint) and an area expansion of 4 between the driver and driven sections. The theoretical and experimental shock velocities produced by the 4000-atm explosive driver studied during this program have been added to this figure to demonstrate the performance of this system relative to other techniques. Results are given for area expansions of 10 and 1 between the driver and driven sections. Experimental data from the electrically heated shock tubes of Jet Propulsion Laboratory (Ref. 8) and AVCO Corporation (Ref. 9) have also been added for purposes of comparison. The driver pressures for these shock tubes are of the order of 1000 atm. The Jet Propulsion Laboratory shock tube has an area expansion of 9 between the driver and driven sections. It can be seen that the shock velocities of this study are considerably higher. Figure 23 also demonstrates the ability of the explosive driver to drive a strong shock wave at constant velocity into a high-pressure test gas.

At the present time a significant effort is being made to improve driver performance by the utilization of electrical energy. However, the use of chemical explosives in shock-tube drivers offers many advantages over the use of electrical energy. Some of the advantages are:

(1) Low-cost energy source and low capital investments in facilities.

(2) High specific energy, on the order of 5000 J/cm^3.

(3) High power output, detonation velocities from 15,000 to 29,000 ft/sec.

(4) Reasonable efficiencies and adequate control of the energy-conversion process between the chemical energy of the explosive and total energy of a gas.

(5) Ability to drive a strong shock at constant velocity into a high-pressure test gas.

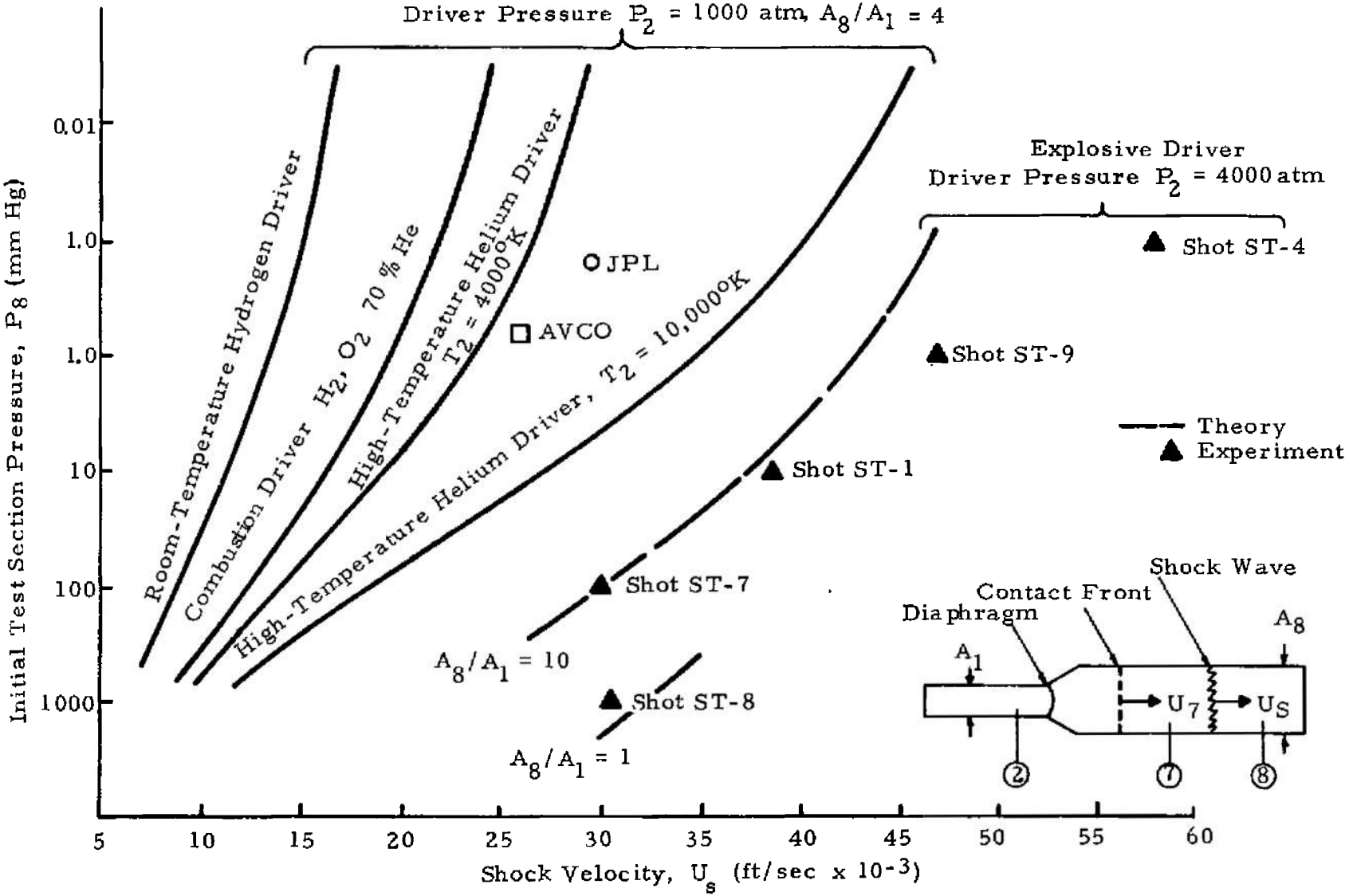

Fig. 23 Performance of Typical Air Shock Tube with Various Drivers

SECTION IV
SUMMARY AND RECOMMENDATIONS

The feasibility of using an explosive driver as the energy source for a high-performance shock tube has been demonstrated. Experiments have shown that the explosive driver is capable of producing strong planar shock waves in air over a wide range of initial gas pressures (1-1000 mm mercury). The best performance in terms of constant shock velocity was 46,910 ft/sec obtained into 1 mm of air. The observed shock velocity and particle velocity agree closely with theoretically predicted values for initial shock tube pressures of 10, 100, and 1000 mm mercury. However, at the lower pressures of 0.1 mm and 1 mm, the experimental shock velocity was significantly greater than that predicted by theoretical calculations. The specific reason for this discrepancy is not completely understood; however, it appears from the photographs of the flow that the shock wave is probably overdriven by a coalescence of waves after the gas emerges from the nozzle.

Reasonable correlation has been obtained between the experimental performance of the explosive driver and that predicted by simple shock-wave theory. The trajectory of the shock wave generated in the explosive driver was found to be quite reproducible. This establishes the controllability of the energy-conversion process between the chemical energy of the explosive and the total energy (kinetic and internal) of the driver gas.

It is recommended that further investigations of the explosive driver be conducted to establish its suitability to an aerodynamic test device. Limited studies should be performed in the following areas:

(1) Optimize the explosive driver and determine the critical design parameters for extending the present range of operation.

(2) Establish the uniformity of the shocked test gas.

(3) Determine the scalability of the explosive driver so that adequate test times can be established.

(4) Measure the flow properties produced by the driver in a single-stage shock tube and compare with theoretical predictions.

(5) Investigate flow properties at high shock-tube pressures using a high-strength driven section to prevent radial expansion.

(6) Minimize the quantity of explosive needed for a given driver to facilitate its use in a permanent shock-tube facility.

(7) Investigate the discrepancies between the observed and predicted flow properties at the lower shock-tube pressures. These discrepancies may be caused by incorrect nozzle expansions or diaphragm openings.

REFERENCES

1. E. T. Moore, D. M. Mumma, C. S. Godfrey, and D. Bernstein, "Explosive Gas Guns for Hypervelocity Acceleration," Proc. of the Fourth Hypervelocity Techniques Symposium, Arnold Engineering Development Center, Tullahoma, Tenn., November 15-16, 1965, 457-484.

2. C. S. Godfrey, "Gas Ejectors for Hypervelocity Projection," Proc. of Seventh Hypervelocity Impact Symposium, Tampa, Fla., November 17-19, 1964, 125-145.

3. J. Hilsenrath and M. Klein, "Tables of Thermodynamic Properties of Air in Chemical Equilibrium Including Second Virial Corrections from 1500°K to 15,000°K," AEDC-TDR-63-161, Arnold Engineering Development Center, Air Force Systems Command, U. S. Air Force, Arnold Air Force Station, Tenn. (August 1963).

4. W. P. Boquist, "Astronomical Photography with the New XR Film," Sky and Telescope (January 1964).

5. J. G. Hall, "Shock Tubes, Part II: Production of Strong Shock Waves; Shock Tube Applications, Design, and Instrumentation," Institute of Aerophysics, University of Toronto, Toronto, Ontario, Canada (May 1958).

6. J. N. Bradley, "Experimental Techniques," Shock Waves in Chemistry and Physics, John Wiley and Sons, New York (1962).

7. W. R. Warren, D. A. Rogers, and C. J. Harris, "The Development of an Electrically Heated Shock Driven Test Facility," General Electric Company, Space Science Laboratory, Missile and Space Vehicle Department, King of Prussia, Penn. (March 1962).

8. D. J. Collins, F. R. Livingston, T. L. Babineaux, and N. R. Morgan, "Hypervelocity Shock Tube," 32-620, Jet Propulsion Laboratory, California Institute of Technology, Pasadena, Calif. (June 15, 1964).

9. P. H. Rose and J. C. Camm, "Electric Shock Tube for High Velocity Simulation," Report 136, AVCO-Everett Research Laboratory, Everett, Mass. (July 1962).

APPENDIX A
DRIVEN TO DRIVER LENGTH REQUIREMENTS

In an explosively driven shock tube, the stopping of the piston produced by the collapse of the driver section produces a rarefaction wave traveling downstream. This wave ultimately overtakes the contact front and destroys the uniform flow behind the incident shock. Under the assemption of an ideal wave system (i.e., planar contact front, uniform flow states, and negligible shock attenuation), an expression may be obtained for the ratio of driven to driver lengths in terms of the computed equilibrium flow properties. It is further assumed that the steady-state expansion, due to the area change, occurs instantaneously at the diaphragm station; that is, the nozzle length is zero. This latter assumption cuases an earlier intersection of the rarefaction wave and contact front than that determined by the inclusion of a finite nozzle length; thus it may in part compensate for the neglect of viscosity.

The assumed wave system, notation, and the velocities of the waves are shown in Figure A-1. The ratio of driven to driver length, L_2/L_1, is given by

$$\frac{L_2}{L_1} = \frac{t_0 U_7}{L_1} = 2\frac{t_C}{t_B}\frac{U_7}{U_{2A}}\frac{x_B/L_1}{(1 - a_{2A}/U_{2A})}$$

where points B, C, and D are defined in Figure A-1 and the origin $x = 0$, $t = 0$ is taken to correspond to normal shock tube notation.

The ratio t_C/t_B, corresponding to the passage of the piston rarefaction wave through the unsteady rarefaction wave produced by the rupture of the diaphragm, is readily determined as

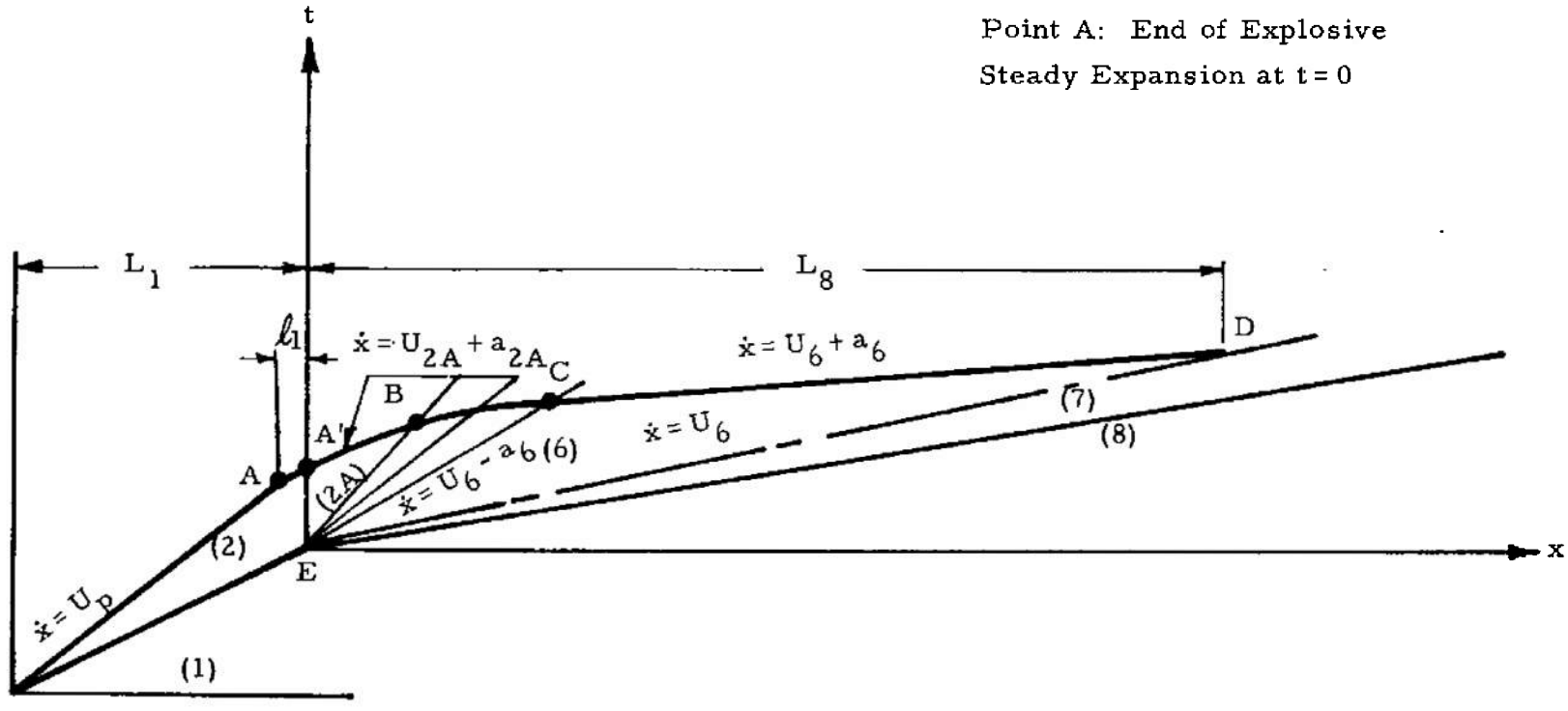

Fig. A-1 Advanced Wave System in an Explosively Driven Shock Tube

$$\frac{t_C}{t_B} = \left(\frac{T_{2A}}{T_6}\right)^{\frac{(\gamma_1 + 1)}{4(\gamma_1 - 1)}}$$

Assuming an instantaneous steady expansion, the ratio x_B/L_1 may be determined by writing

$$t_B = \frac{x_B}{U_{2A} - a_{2A}} = t_A + \frac{x_B}{U_{2A} + a_{2A}}$$

which yields

$$\frac{x_B}{L_1} = \frac{1}{2} \frac{U_{2A}^2}{U_p U_{2A}} \left[1 - \left(\frac{a_{2A}}{U_{2A}}\right)^2\right]\left[1 - \frac{U_p}{U_s} - \frac{\ell_1}{L_1}\left(\frac{1}{1 + U_p/a_s}\right)\right]$$

Utilizing the ideal gas in state (2) and the strong shock approximation for U_p/U_s, the ratio of required driven to driver length is

$$\frac{L_2}{L_1} = \frac{U_7}{U_p}\left(1 + \frac{U_{2A}}{a_{2A}}\right)\left(\frac{T_{2A}}{T_6}\right)^{\frac{(\gamma_1 + 1)}{4(\gamma_1 - 1)}}\left[\frac{\gamma_1 - 1}{\gamma_1 + 1} - \frac{\ell_1}{L_1}\left(\frac{1}{1 + U_p/a_2}\right)\right]$$

Security Classification

DOCUMENT CONTROL DATA - R&D

(Security classification of title, body of abstract and indexing annotation must be entered when the overall report is classified)

1 ORIGINATING ACTIVITY (Corporate author)	2a REPORT SECURITY CLASSIFICATION
Physics International Company 2700 Merced Street San Leandro, California	UNCLASSIFIED
	2b GROUP N/A

3 REPORT TITLE

EXPLOSIVELY DRIVEN SHOCK TUBES

4 DESCRIPTIVE NOTES (Type of report and inclusive dates)

Final Technical Report Period Covered: August 1965-June 1966

5 AUTHOR(S) (Last name, first name, initial)

Moore, E. T., Jr., Physics International Company

6. REPORT DATE	7a. TOTAL NO. OF PAGES	7b. NO OF REFS
November 1966	51	9

8a CONTRACT OR GRANT NO.	9a ORIGINATOR'S REPORT NUMBER(S)
AF40(600)-1139 b. PROJECT NO. 7778 c. Program Element 62410034 d. Task 777807	AEDC-TR-66-238
	9b. OTHER REPORT NO(S) (Any other numbers that may be assigned this report) PIFR-037

10 AVAILABILITY/LIMITATION NOTICES

This document is subject to special export controls and each transmittal to foreign governments or foreign nationals may be made only with prior approval of Arnold Engineering Development Center.

11. SUPPLEMENTARY NOTES	12. SPONSORING MILITARY ACTIVITY
Available in DDC	Arnold Engineering Development Center Air Force Systems Command Arnold Air Force Station, Tennessee

13 ABSTRACT

This report summarizes the analytical and experimental effort that demonstrates the feasibility of using an explosive driver to produce strong planar shock waves at constant velocity in air. Shock-tube performance using an explosive driver was experimentally investigated for initial test gas pressures ranging from 0.1 mm Hg to 1000 mm Hg. The best performance in terms of constant shock velocities was 46,900 ft/sec obtained in 1.0 mm Hg of air.

This document has been approved for public release [illegible]

Per AFSC Ltr dtd 12 Feb 73
signed by Wallace O. Cole

DD FORM 1 JAN 64 1473

Security Classification

Security Classification

14 KEY WORDS	LINK A		LINK B		LINK C	
	ROLE	WT	ROLE	WT	ROLE	WT
1. shock tubes -- Feasibility						
~~shock waves~~						
2 shock tunnels --						
hypervelocity						
hypervelocity phenomena						
hypervelocity flow						
explosive						
3 explosive ~~device~~ driven						
supersonic flow						
4 Explosively driven shock tube						

17-3

INSTRUCTIONS

1. ORIGINATING ACTIVITY: Enter the name and address of the contractor, subcontractor, grantee, Department of Defense activity or other organization *(corporate author)* issuing the report.

2a. REPORT SECURITY CLASSIFICATION: Enter the overall security classification of the report. Indicate whether "Restricted Data" is included. Marking is to be in accordance with appropriate security regulations.

2b. GROUP: Automatic downgrading is specified in DoD Directive 5200.10 and Armed Forces Industrial Manual. Enter the group number. Also, when applicable, show that optional markings have been used for Group 3 and Group 4 as authorized

3. REPORT TITLE: Enter the complete report title in all capital letters. Titles in all cases should be unclassified. If a meaningful title cannot be selected without classification, show title classification in all capitals in parenthesis immediately following the title.

4. DESCRIPTIVE NOTES: If appropriate, enter the type of report, e.g., interim, progress, summary, annual, or final. Give the inclusive dates when a specific reporting period is covered.

5. AUTHOR(S): Enter the name(s) of author(s) as shown on or in the report. Enter last name, first name, middle initial. If military, show rank and branch of service. The name of the principal author is an absolute minimum requirement.

6. REPORT DATE: Enter the date of the report as day, month, year, or month, year. If more than one date appears on the report, use date of publication.

7a. TOTAL NUMBER OF PAGES: The total page count should follow normal pagination procedures, i.e., enter the number of pages containing information.

7b. NUMBER OF REFERENCES: Enter the total number of references cited in the report.

8a CONTRACT OR GRANT NUMBER: If appropriate, enter the applicable number of the contract or grant under which the report was written.

8b, 8c, & 8d. PROJECT NUMBER: Enter the appropriate military department identification, such as project number, subproject number, system numbers, task number, etc.

9a. ORIGINATOR'S REPORT NUMBER(S). Enter the official report number by which the document will be identified and controlled by the originating activity. This number must be unique to this report.

9b. OTHER REPORT NUMBER(S): If the report has been assigned any other report numbers *(either by the originator or by the sponsor)*, also enter this number(s).

10. AVAILABILITY/LIMITATION NOTICES: Enter any limitations on further dissemination of the report, other than those imposed by security classification, using standard statements such as:

(1) "Qualified requesters may obtain copies of this report from DDC."

(2) "Foreign announcement and dissemination of this report by DDC is not authorized."

(3) "U. S. Government agencies may obtain copies of this report directly from DDC. Other qualified DDC users shall request through _____."

(4) "U. S. military agencies may obtain copies of this report directly from DDC. Other qualified users shall request through _____."

(5) "All distribution of this report is controlled. Qualified DDC users shall request through _____."

If the report has been furnished to the Office of Technical Services, Department of Commerce, for sale to the public, indicate this fact and enter the price, if known.

11. SUPPLEMENTARY NOTES: Use for additional explanatory notes.

12. SPONSORING MILITARY ACTIVITY: Enter the name of the departmental project office or laboratory sponsoring *(paying for)* the research and development. Include address.

13. ABSTRACT: Enter an abstract giving a brief and factual summary of the document indicative of the report, even though it may also appear elsewhere in the body of the technical report. If additional space is required, a continuation sheet shall be attached.

It is highly desirable that the abstract of classified reports be unclassified. Each paragraph of the abstract shall end with an indication of the military security classification of the information in the paragraph, represented as *(TS), (S), (C), or (U)*

There is no limitation on the length of the abstract However, the suggested length is from 150 to 225 words.

14 KEY WORDS: Key words are technically meaningful terms or short phrases that characterize a report and may be used as index entries for cataloging the report Key words must be selected so that no security classification is required. Identifiers, such as equipment model designation, trade name, military project code name, geographic location, may be used as key words but will be followed by an indication of technical context. The assignment of links, rules, and weights is optional.

Security Classification